Idempotent Statistics of the Motzkin, Jones and Kauffman Monoids

Igor Dolinka, James East, Athanasios Evangelou , Desmond FitzGerald , Nicholas Ham , James Hyde, Nicholas Loughlin

January 13, 2016

Abstract

We describe a refinement of the natural partial order on the set of idempotents of the Motzkin monoid of general degree n which exhibits its structure as a disjoint union of geometric complexes. This leads to an efficient method for computing the numbers of idempotents and their distribution across ranks. The method extends to idempotent numbers in the Jones (or Temperley-Lieb) and Kauffman monoids. Values are tabulated for monoids of small degree in all three of these families. Ramifications are discussed in the case of the Jones monoids, and include recurrence relations involving exotic Catalan-like return statistics and connexions with meandric numbers.

Mathematics Subject Classification 2010: 05E15, 05A18, 20M20.

1 Introduction

The 'statistics' of the title is intended in the sense of population statistics. That is, our concern is with evaluation of the number of idempotents ($x^2 = x$) in certain monoids (semigroups with identity) which we describe below, and the distribution of these numbers according to rank or other parameters. The monoids involved are planar diagram monoids, which is to say, submonoids of a partition monoid whose elements are planar when using the conventional representation of the partition monoid in the Cartesian plane. The planar constraint, which may also be described as a non-crossing condition, implies that all subgroups of these monoids are trivial. The idempotents in a semigroup are precisely its trivial subgroups, so one of our main purposes in this study is to better understand these monoids through the 'spatial' distribution of their subgroups.

The particular monoids we consider are the well-studied Jones monoids, also called Temperley-Lieb monoids, and their extensions, the Motzkin monoids. Each of these names refers to a sequence of monoids, one for each natural number (the cardinality of an underlying set), and so we are concerned with sequences of integers. Thus another main purpose of our study is to identify these sequences, and make connexions with related sequences where possible.

This paper is a complement and companion to the paper [4] which gave formulæ for the numbers of idempotents in the partition monoid on n vertices and in several of its subsemigroups and in bases of their associated algebras[1]. However the methods employed in the paper in hand are necessarily different: the planarity constraint means that the set symmetries used to study the semigroups in [4] are no longer available, and we suspect that enumeration of the planar idempotents becomes inimical to closed-form solution. Indeed, enumeration of idempotents of

[1] Richard Mathar has pointed out an error in Table 2 of [4]: $c(\mathscr{PB}_n) = 725\,\mathbf{760}$ at $n = 9$.

the Jones monoid has been posed as an open problem [11]. We address this problem by presenting methods for computing the numbers of idempotents in the Motzkin and Jones monoids, with attention given to efficiency of the algorithms involved in terms of their time and space complexities. We also show that recurrences for the sequence of idempotent counts in the Jones monoids involve complex statistics of Dyck paths, and argue that this supports the claim that enumeration of idempotents in these planar monoids is a difficult problem.

The paper is organised as follows. In Section 2, we describe the elements of the Motzkin and Jones monoids and their product rule, and characterise the idempotents. Section 3 is the core of the paper, describing a method for counting the idempotents in these monoids by reducing the problem to statistics associated with low-rank idempotents. Following sections refine the method, examine the twisted variants of the monoids, and discuss the implementation of the method. Tables of values are presented for small numbers of vertices, and we conclude with a closer examination of the Jones monoid including recurrence relations (with exogenous terms) for the Jones counts.

The reader is referred to the monographs of Howie [10] and Higgins [9] for background on semigroups in general, and to the introduction to the present authors' article [4] and references contained therein—in particular, to foundational articles of Martin [18] and Halverson and Ram [7]—for background and relevant detail on the partition, Brauer and partial Brauer monoids.

2 Preliminaries

We will be dealing with the planar parts of the following monoids discussed in [4]: the partition monoid $\mathscr{P}_n$, the Brauer monoid $\mathscr{B}_n$, and the partial Brauer monoid $\mathscr{PB}_n$, all on n vertices. (Of course we will only discuss semigroups over finite sets X, and hence write $\mathscr{P}_n$ for $\mathscr{P}_X$, etc.) So we begin with a short definition of $\mathscr{P}_n$, and simple explanations of the processes of extending a submonoid of $\mathscr{P}_n$ by partialisation, and of selecting *planar* elements into a submonoid. If this sounds too nebulous to some readers, and to others too pedantic, then we shall claim to have struck a happy medium.

Let $\mathbb{N}_n = \{1, \dots n\}$ and consider the point sets in $\mathbb{R}^2$ given by

$$X = \{(i, 1) : i \in \mathbb{N}_n\}, \quad X' = \{(i, 0) : i \in \mathbb{N}_n\}.$$

We think of X as the set of *upper vertices*, and X' as the set of *lower vertices*. These (concrete) sets will be used to form elements of the partition monoid $\mathscr{P}_n$ in the manner described for abstract sets in [4]. That is, an element α of $\mathscr{P}_n$ is simply a partition of $X \cup X'$ in the sense of set theory. As in [4], we may think of each component of the partition α as a complete graph on its vertices, but represent it pictorially by showing any of its spanning trees. Examples may be given using an obvious shorthand, in which (say) the partition $\{1, 2, 4, 3'\}, \{3, 1', 2'\}, \{4'\}$ of three components on 8 vertices ($n = 4$) may be drawn as 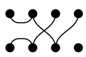. Since the value of n will be fixed in any context, we will mostly regard these graphs as sets of edges, and thus containment will refer to these edge-sets.

Elements of $\mathscr{P}_n$ are composed in the way described in [4] or earlier references therein. For completeness, we repeat the description here, using the concrete description of plane point sets above. Let $\alpha, \beta \in \mathscr{P}_n$. Consider a third point set $X'' = \{(i, -1) : i \in \mathbb{N}_n\}$. Leave α as a graph on $X \cup X'$, and replace β by a copy of itself on $X' \cup X''$ by translating β downwards, $(x, y) \mapsto (x, y - 1)$. We now have a graph $\alpha + \beta$ (possibly with multiple edges) on $X \cup X' \cup X''$. Let G be its transitive closure, so that an edge of G corresponds to a path in $\alpha + \beta$. In this graph G, we refer to the vertices of X' as the *interface*. Finally, the product $\alpha\beta$ is the induced subgraph of G on the vertex set $X \cup X''$—or more properly, the result of mapping this back to the canonical vertex set $X \cup X'$ by the translation-compression $(x, y) \mapsto (x, \frac{y+1}{2})$. This means that the vertices of the interface are omitted, as is any component of $\alpha + \beta$ entirely within the interface; such a component will be called a *floating* component. A sample calculation is given in Figure 1.

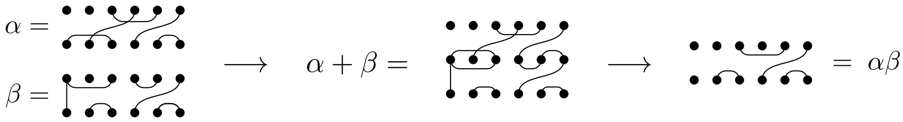

Figure 1: Two partitions $\alpha, \beta \in \mathscr{P}_6$ (left), the construction $\alpha + \beta$, and the product $\alpha\beta \in \mathscr{P}_6$ (right).

A component of $\alpha \in \mathscr{P}_n$ is *transversal* if it contains both an upper vertex and a lower vertex, and the number of transversals of α is called the *rank* of α and denoted by $\operatorname{rank}(\alpha)$. The set of those $\alpha \in \mathscr{P}_n$ such that each component has cardinality 2 (that is, α is a perfect matching) is closed under the product in $\mathscr{P}_n$, and known as the *Brauer* monoid $\mathscr{B}_n$. An example of $\alpha \in \mathscr{B}_n$ with $n = 4$ has components $\{1, 1'\}, \{2, 3\}, \{2', 4'\}, \{3', 4\}$ and is depicted in the graph 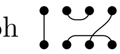; its transversals are $\{1, 1'\}$ and $\{3', 4\}$.

A *partial version* of any $\alpha \in \mathscr{P}_n$ is a member of $\mathscr{P}_n$ obtained by the deletion of any subset of the edges of α. For example, the graph 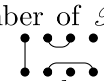 is a partial version of 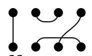 above. If S is a subsemigroup of $\mathscr{P}_n$, we define the *partial version* of S to consist of all partial versions of all $s \in S$, and denote it by $\mathscr{P}S$. (Clearly $S \subseteq \mathscr{P}S = \mathscr{P}\mathscr{P}S$, $\mathscr{P}\mathscr{P}_n = \mathscr{P}_n$ and in fact $\mathscr{P}_n = \mathscr{P}\{\zeta\}$ where ζ is the partition of one component—the complete graph—on $2n$ vertices.) If $\alpha, \beta \in S \subseteq \mathscr{P}_n$ and γ, δ are partial versions of α, β respectively, then (as is easily seen) $\gamma\delta$ is a partial version of $\alpha\beta$; thus $\mathscr{P}S$ is a subsemigroup of $\mathscr{P}_n$ which contains S, and is a submonoid if S is.

At this point we need the concrete description to define planarity. This could also be termed a *non-crossing* condition, but the reference to planarity sits better with our use of graphical terms. An element $\alpha \in \mathscr{P}_n$ is called *planar* if there is a way of drawing its edges in $\mathbb{R}^2$, entirely within the convex hull of $X \cup X'$, the rectangle $[1, n] \times [0, 1] \subset \mathbb{R}^2$ formed by the upper and lower vertices, so that no two edges intersect. For a subsemigroup S of $\mathscr{P}_n$, let πS denote the set of its planar members. Now $\pi S = S \cap \pi\mathscr{P}_n$ and it is clear from the definition that if α, β are planar, then so too is $\alpha\beta$; thus πS is a subsemigroup of S, and a submonoid of $\mathscr{P}_n$ if S is. Of the graphical examples above, 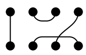 is non-planar, and 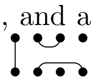 is not only a member of the partial Brauer monoid but also planar; 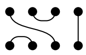 gives us an example of a planar member of $\mathscr{B}_n$, thus a member of $\pi\mathscr{B}_n$.

We consider the planar parts of the three kinds of monoid studied in [4], which is to say, $\pi\mathscr{B}_n \subseteq \pi\mathscr{P}\mathscr{B}_n \subseteq \pi\mathscr{P}_n$. The first, $\pi\mathscr{B}_n$, is known by the names *Jones* monoid or *Temperley-Lieb* monoid, here denoted by $\mathscr{J}_n$. The monoid $\mathscr{J}_n$ (and its twisted version the Kauffman monoid $\mathscr{K}_n$, which we discuss later) first emerged as bases of the Temperley-Lieb algebras. These algebras were studied by their eponyms in connection with lattice spin problems [21] and later, as a hyperfinite II_1 factor of a von Neumann algebra, in Jones's papers [12, 13]. In both cases the definitions were by generators and relations, but later Kauffman popularised the representation by diagrams. Only later did its over-semigroup $\mathscr{P}_n$ came to prominence through the work of Martin [18]. The second kind of monoid $\pi\mathscr{P}\mathscr{B}_n$ has been studied by Benkart and Halverson [1] as a basis for the Motzkin algebra, and named the *Motzkin* monoid $\mathscr{M}_n$ because of its connection with Motzkin numbers. The third kind, the *planar partition* monoid $\pi\mathscr{P}_n$ was shown by Halverson and Ram [7] to be isomorphic to $\mathscr{J}_{2n}$. So we need to consider $\mathscr{J}_n = \pi\mathscr{B}_n$ and $\mathscr{M}_n = \pi\mathscr{P}\mathscr{B}_n$.

We remark that intermediate between these two lies the *partial Jones* monoid $\mathscr{PJ}_n = \mathscr{P}\pi\mathscr{B}_n$—here is an example with $n = 4$: 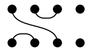 $\in \mathscr{PJ}_n \setminus \mathscr{J}_n$. In fact, both containments are proper for $n \geq 2$—for example, 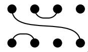 $\in \mathscr{M}_n \setminus \mathscr{PJ}_n$ since the only possible completion to a complete matching would involve a crossing. Our present methods do not succeed for this monoid $\mathscr{PJ}_n$, so we omit it from analysis in later sections. Our exposition begins with $\mathscr{M}_n$, because many facts specialise easily to $\mathscr{J}_n$.

2.1 Representations of Motzkin elements

The graphical description of the elements of $\mathscr{M}_n$ as given above is good for working with the multiplication operation, but less useful for other purposes such as listing, enumerating, or checking for idempotency. So we shall describe other representations of Motzkin elements. Most of these are quite well known for the Jones elements, but less so for the more general kind.

(i) By our definition above, elements of $\mathscr{M}_n$ are Brauer diagrams with some (or no) edges removed, so that they are planar diagrams in which each component has cardinality one or two. There is an 'unfolding' process familiar in the Jones context: let the vertices be read in the order $1, \ldots n, n', (n-1)', \ldots 1'$, and interpret each edge as a pair of brackets, leaving the isolated vertices alone. This shows that a Motzkin element is represented as a *partial bracketing* on $2n$ vertices, which is to say, a well-formed string of s pairs of brackets ($s \leq n$) interspersed by an even number $2n - 2s$ of dots (the isolated vertices). In the case of 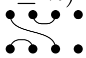 above, the corresponding partial bracketing is $(()\cdot\cdot)()$, and for 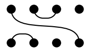, it is $(()\cdot)\cdot()$. If there are no isolated vertices, the given bracketing represents an element of the Jones monoid, as is the case for 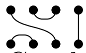, represented by $(()())()$. As a consequence of this representation, we have that $|\mathscr{J}_n| = C_n$, the n-th Catalan number. If the isolated vertices can be replaced by pairs of matched brackets to make a well-formed bracketing, then the string of brackets and dots represents a member of the partial Jones monoid, as does 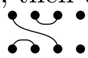 but not 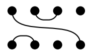 or 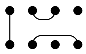.

(ii) A second representation of a Motzkin element is as a *Motzkin word* of length $2n$, that is, a sequence $\{x_i\}$, $i = 1, \ldots 2n$ over $\{-1, 0, +1\}$ with partial sums $z_r := \sum_1^r x_i \geq 0$ and $z_{2n} = 0$, where $+1$ corresponds to a left bracket, -1 to a right, and 0 to a lone vertex. These are discussed in [1] and they are often also encoded as U, D and F respectively (for *up, down* and *flat*). We switch freely between these symbols: for example,  maps to $(+1, +1, -1, 0, 0, -1, +1, -1)$ or $UUDFFDUD$. It follows as seen in [1] that $|\mathscr{M}_n|$ is the $2n$-th Motzkin number, appearing in the OEIS [20] as sequence A026945 and as a subsequence of A001006. In this representation, $\{i, j\}$ is a transversal of α if $\{i, j\}$ is an edge with $i \leq n < j$, (for example, $\{1, 6\}$ in 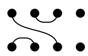).

(iii) A third representation is as a sequence of partial sums of the above, that is a sequence $\{z_i \colon 0 \leq i \leq 2n\}$ of length $2n + 1$ over $\mathbb{N}$ with $z_0 = z_{2n} = 0$ and $|z_{i+1} - z_i| \leq 1$. For example,  codes as $(0, 1, 2, 1, 1, 1, 0, 1, 0)$. It is easy to see how to move between the first and second, and between the second and third representations. Here is a recipe for reconstructing the original graph directly from (iii): Given a representation as in (iii), define a graph on $\mathbb{N}_{2n}$ as follows. For vertex i, recover x_i by $x_i = z_i - z_{i-1}$, and define the *level* at vertex i as $\ell_i = \min\{z_{i-1}, z_i\}$. Then $\{i, j\}$ is an edge if and only if $x_i = 1, x_j = -1$, and j is the least index $> i$ such that $\ell_i = \ell_j$. The edge $\{i, j\}$ is also said to be a *return at level* ℓ_i, and a return at level 0 is usually called simply a *return*. The levels of example 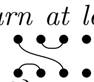 $= (0, 1, 2, 1, 1, 1, 0, 1, 0)$ are $(0, 1, 1, 1, 1, 0, 0, 0)$, and edges recovered as $\{1, 6\}, \{2, 3\}, \{7, 8\}$—or, in original notation, $\{1, 3'\}, \{2, 3\}, \{2', 1'\}$. At this point, we may note that each transversal edge has a unique level, and that transversals are ordered left to right by their levels.

Let us pause here for two examples which are more extensive. Consider the element of $\mathscr{M}_8$

depicted by

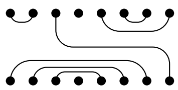

Properties and quantities defined above are tabulated in the first seven rows of Table 1 (above the line). Observe that there are seven edges, of which three are returns, including one transversal at level zero.

Table 1: Computation of various quantities for an example in $\mathscr{M}_8$. Edges are labeled by their first-encountered incident vertex, and components are labeled by the least index they contain. Key: Comp. = component; C = cycle, TA = trans-active path, I = inert path.

Orig. vx		1	2	3	4	5	6	7	8	$8'$	$7'$	$6'$	$5'$	$4'$	$3'$	$2'$	$1'$
Index i	0	1	2	3	4	5	6	7	8	9	10	11	12	13	14	15	16
Rep. (ii) x_i		1	-1	1	0	1	1	-1	-1	-1	1	1	1	0	-1	-1	-1
Rep. (iii) z_i	0	1	0	1	1	2	3	2	1	0	1	2	3	3	2	1	0
Level ℓ_i		0	0	0	1	1	2	2	1	0	0	1	2	3	2	1	0
Edge label		1	1	3	-	5	6	6	5	3	$7'$	$6'$	$5'$	-	$5'$	$6'$	$7'$
(0-)return		Y	Y	Y						Y	Y						Y
Comp. label		1	1	3	4	3	1	1	3	3	1	1	3	4	3	1	1
Comp. type		C	C	TA	I	TA	C	C	TA								
u_θ		1	1														
ℓ_θ							1	1									

An example from $\mathscr{M}_{15}$ may be similarly instructive:

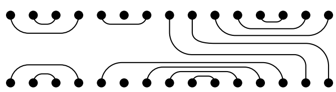

Here we see two transversals $\{8, 14'\}$—the leftmost, at level 0—and $\{9, 15'\}$, at level 1. Non-transversal return edges are $\{1, 4\}$, $\{5, 7\}$, $\{1', 4'\}$ and $\{5', 13'\}$; note they are to the left of the transversal of level 0. We return to these examples later on.

(iv) A fourth representation of $\alpha \in \mathscr{M}_n$, clearly equivalent to (ii), is as a pair of words of length n. Let $y_i = -x_{2n+1-i}$ for $i = 1 \dots n$. Then, still with $i = 1 \dots n$, each of $\mathbf{x} = (x_i)$ and $\mathbf{y} = (y_i)$ is a *Motzkin semi-word*, defined as for Motzkin words but satisfying the inequalities $\sum_1^n x_i,\ \sum_1^n y_i \geq 0$, and the pair $(\mathbf{x}, \mathbf{y})$ is a *matched pair* in that $\sum_1^n x_i = \sum_1^n y_i$. This common value is rank(α). In representation (iv), 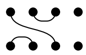 becomes $(UUDF, UDUF)$ (note reversal of order and sign for $\mathbf{y}$).

In representations (ii), (iii) and (iv), the element is in $\mathscr{J}_n$ if and only if the word has no flats ($x_i \neq 0$ for all i), and if a Motzkin semi-word has no flats, we shall name it a *Dyck semi-word.* For a Motzkin or Dyck semi-word $\mathbf{x}$, the pair $(\mathbf{x}, \mathbf{x})$ represents a *projection* (symmetric idempotent), and every projection is represented in this manner. Our examples 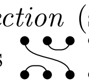, 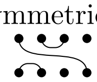, and 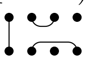 are all of rank 1, and all of the form $(UUDF, \cdots)$, sharing the same left semi-word; the symmetrical element with this left semi-word is $(UUDF, UUDF)$, which is 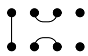 in graphical form.

The representation (iv) is related to the algebraic structure of $\mathscr{M}_n$—the left [right] semi-words index the classes of Green's relation $\mathscr{R}$ [$\mathscr{L}$]—and this yields some enumeration results. In $\mathscr{M}_n$ and $\mathscr{J}_n$, elements are $\mathscr{D}$-equivalent if and only if they have the same rank. Moreover, each element is uniquely determined by a matched pair of Motzkin semi-words [1]. Let $U_{n,k}$ [$T_{n,k}$] denote the number of Motzkin [Dyck] semi-words of length n and rank k; then the size of the

$\mathscr{D}$-class of rank k in $\mathscr{M}_n$ [$\mathscr{J}_n$] is $U_{n,k}^2$ [$T_{n,k}^2$] and so

$$|\mathscr{M}_n| = M_{2n} = \sum_{k=0}^{n} U_{n,k}^2 \text{ and } |\mathscr{J}_n| = C_n = \sum_{k=0}^{n} T_{n,k}^2.$$

Clearly, $T_{n,k} = 0$ unless $k \equiv n \pmod 2$. By definition, $U_{n,0} = M_n$, giving the (odd and even) Motzkin numbers appearing as A001006 in the OEIS [20]; and $T_{2k,0} = C_k = T_{2k-1,1}$, the Catalan numbers. The triangular array $T_{n,k}$ is A008313, also the Catalan triangle with rows read in reverse order; similarly the array $U_{n,k}$ is A064189, the Motzkin triangle (A026300) in reverse row order. The respective row sums are given by A005773 ($\sum_k U_{n,k}$) and the central binomial coefficients ($\sum_k T_{n,k}$). These latter sequences also give the total number of projections in $\mathscr{M}_n$ [$\mathscr{J}_n$], since the number of projections of rank k in $\mathscr{M}_n$ [$\mathscr{J}_n$] is $U_{n,k}$ [$T_{n,k}$].

(v) A fifth representation of a Motzkin element is of such importance to our results that the next subsection is devoted to describing it. It may be visualised as an extension of the 'unfolding trick' found in (i), in which the unfolding, a rotation through angle π, is continued through a further angle π so that the upper and lower vertex positions coincide, and the transversal edges are then 'pruned'. This results in the upper and lower vertex sets coinciding, their edges distinguished by lying on opposing sides of the row of coalesced vertices. A formal description begins the next section.

2.2 Kernels and interface graphs

In [4] we used the notion of a *kernel* of an element $\alpha \in \mathscr{P}_n$ and its graphical variant $\Gamma(\alpha)$. The latter was described in Section 2 of [4], and applied to $\mathscr{PB}_n$ where we have simplification arising from the fact that every component of α has at most two vertices. We now specialise this notion for the Motzkin monoid, when the extra condition of planarity holds. We will have frequent occasion to refer to these, and name them *interface graphs*, since they are precisely the graphs arising at the interface between two copies of α when they are multiplied to form α^2. The vertex set of an interface graph is (a copy of) $X' = \{(i, 0) : i \in \mathbb{N}_n\}$, and on this we draw, 'below the line', a copy of the subgraph of α induced on X, and 'above the line' we draw a copy of the subgraph of α induced on X'. Vertices belonging to a transversal edge of α will be distinguished graphically in $\Gamma(\alpha)$ by putting short line segments on the vertices in the appropriate directions; we think of these as decorations on the vertices and not as edges.

As examples, let us present by interface graphs some of the elements discussed previously. In order we have $\Gamma($ 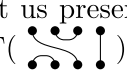 $)=$ , $\Gamma($ 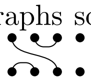 $)=$  , $\Gamma($ 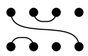 $)=$ , and $\Gamma($ 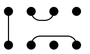 $)=$ 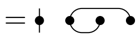 .

We need to distinguish different kinds of vertices and edges in α and $\Gamma(\alpha)$. If a vertex belongs to a transversal edge of α, it is said, in $\Gamma(\alpha)$, to be *active downwards* if in X, and *active upwards* if in X'. If a vertex is a singleton component of α, it is said to be *inert downwards* if in X, and *inert upwards* if in X'. Referring once more to our examples, in , vertex 1 is active downwards, 3 active upwards, and 4 active in both directions;  has vertex 4 inert both up- and downwards;  has vertex 3 inert upwards, and 4 active upwards and inert downwards; and 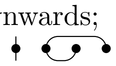 has 1 active in both directions, 3 inert upwards and 4 inert downwards. We shall extend a convention that was used above for vertices, and refer to edges in $\Gamma(\alpha)$ as either lower (dashed) or upper (undashed). Note that the *upper* edges *descend* from the vertices in an interface graph, while lower edges ascend!

We do not need to characterise interface graphs, but it is useful to observe that the construction of $\Gamma(\alpha)$ from α is readily reversed. First copy the downward edges and decorations to X and the upward edges and decorations to X'. Then (by the planarity constraint) there is only one way to draw edges incident on active vertices to recover α. (The vertices of $\Gamma(\alpha)$ which are active upwards have levels $0, \ldots, \mathrm{rank}(\alpha) - 1$ and so do the vertices which are active downwards. Thus α is recovered by simply joining the active vertices of equal rank.)

Each $\Gamma(\alpha)$ is of course a disjoint union of connected components (called Γ-*components* to distinguish them from components of the graphical α); the *length* of a component is the number of edges it contains. Each Γ-component is either a cycle (of positive even length) or a path (including singleton vertices, regarded as of length 0). The terminology for vertices above carries over to paths in $\Gamma(\alpha)$ as follows: we say a path is *active* or *inert* according as both endpoints are active or inert respectively, and otherwise we say the path is *mixed*, that is, when one terminus is active and the other inert. If a path is of odd length, then we call it *cis*, since the termini face to the same side of the interface; if it is of even length, then we call it *trans*, because the termini face toward opposite sides of the interface. A trans-active path in $\Gamma(\alpha)$ corresponds to a transversal edge in the pictorial α. When we speak of return edges in $\Gamma(\alpha)$, we mean (unless otherwise specified) those contained in cycles.

Let us illustrate these concepts by reference to the larger examples seen above. The element on 8 vertices, picked apart in Table 1, has the following interface graph:

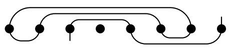
.

It has a trans-active path of length 2 on vertices $3, 5, 8$, an inert path of length 0 on vertex 4, and a cycle of length 4 on remaining vertices. Return edges contained in cycles are $\{1, 7\}$ (lower or upwards) and $\{1, 2\}$ (upper or downwards). The transversal return edge $\{3, 8'\}$, evident previously, is merely implicit in the decorations on vertices 3 and 8. These quantities are shown in Table 1, each return edge being marked twice.

The element on 15 vertices has interface graph

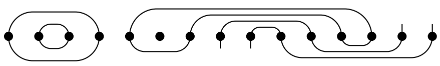
,

with both upper and lower return edges on $\{1, 4\}$, an upper return on $\{5, 7\}$ and a lower return on $\{5, 13\}$. Its components are three cycles and three paths. Two of the paths are trans-active, with implied transversal edges at levels 0 and 1, and one path is inert and of length 0.

2.3 Characterisation of idempotents

An element s of a semigroup S is an *idempotent* if $s^2 = s$; the set of idempotents in a subset X of S will be denoted by $E(X)$.

We saw above that $\Gamma(\alpha)$ encodes α. Our first result exploits the fact that it also encodes α^2.

Proposition 2.1. Let $\alpha \in \mathscr{M}_n$. Then $\alpha = \alpha^2$ if and only if each component of $\Gamma(\alpha)$ is either a cycle, an inert path, or a trans-active path.

Proof. The interface graph $\Gamma(\alpha)$ is the middle layer in the construction $\alpha + \alpha$ used to define the product α^2. Suppose $\Gamma(\alpha)$ contains a mixed path with one terminus i' a vertex active upwards and the other terminus j' inert. Then i' is in a transversal edge ki' (say) of the upper factor α, while k is in no transversal of α^2. Thus $\alpha^2 \neq \alpha$. Similarly for a mixed path with one terminus active upwards. Now suppose $\Gamma(\alpha)$ contains a path with both termini i', j' active upwards. Then there are transversal edges of α, ki' and lj' say, which are not in α^2 because it has an edge kl. Similarly for termini active downwards. Thus if $\alpha = \alpha^2$ then $\Gamma(\alpha)$ can have no mixed paths and no cis-active paths.

Conversely if the only active vertices of $\Gamma(\alpha)$ occur in pairs as upward- and downward-facing termini of a trans-active path, then by planarity (non-crossing) these paths may be labeled

$0, \ldots, \mathrm{rank}(\alpha) - 1$ (in agreement with the levels of the corresponding transversals of α). Consider the termini of such a path, say i' active upwards and j' active downwards. Then ji' and $j'i''$ are edges in $\alpha + \alpha$. It follows that α and α^2 have the same transversals. Since they also have the same no-transversal edges, they are equal. □

With this criterion it is easy to check that amongst our examples with $n = 4$, , 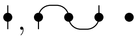, and 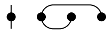 are all idempotent, while  is not, because of its mixed paths. The exemplars from $\mathscr{M}_8$ and $\mathscr{M}_{15}$ are idempotent. There is a simplification of the criterion for Jones elements:

Corollary 2.2. Let $\alpha \in \mathscr{J}_n$. Then α is an idempotent if and only if its interface graph $\Gamma(\alpha)$ has no odd path. □

Some understanding of the overall structure of a semigroup may be had from its *eggbox diagram* [10]. In an eggbox diagram, elements of the semigroup are placed in the same column [resp. row] if they generate the same left [right] ideal. A non-empty intersection of a row and a column is called an $\mathscr{H}$-class, and every $\mathscr{H}$-class contains at most one idempotent. The relation $\mathscr{D}$ is defined as the join of the equivalence relations $\mathscr{R}$ and $\mathscr{L}$ defined by common row and column membership respectively, and the whole complex is sometimes referred to as the $\mathscr{D}$*-structure* of the semigroup. The eggbox diagram of S may be used to show what we referred to above as the spatial distribution of idempotents in S.

If S is a subsemigroup of $\mathscr{P}_n$, we write $D_r(S)$ (or just D_r if the meaning is clear) for the subset of S consisting of elements of rank (number of transversals) r; for $S = \mathscr{P}_n$, $S = \mathscr{M}_n$ or $S = \mathscr{J}_n$. We shall be particularly interested in the properties of D_r where $r \in \{0, 1\}$ because, as we see in the next section, all idempotents of $\mathscr{M}_n$ and $\mathscr{J}_n$ may be developed from idempotents in these classes. The $\mathscr{D}$-class of lowest rank is made up entirely of idempotents. For convenience we write $D = E(D_0 \cup D_1) = D_0 \cup E(D_1)$. Note that $D_r(\mathscr{J}_n) = \emptyset$ unless $r \equiv n \pmod 2$, so $D(\mathscr{J}_n) = D_{n \bmod 2}(\mathscr{J}_n)$. However $D(\mathscr{M}_n) = D_0(\mathscr{M}_n) \cup E(D_1(\mathscr{M}_n))$, since $D_0(\mathscr{M}_n)$ is never empty and $D_1(\mathscr{M}_n)$ contains non-idempotents for $n \geq 2$.

Figure 2 illustrates these concepts. It depicts the eggbox diagram for the $\mathscr{D}$-classes of $\mathscr{M}_4$ of ranks 0 and 1, with elements portrayed using interface graphs. The $\mathscr{L}$- and $\mathscr{R}$-classes (rows and columns of the egg-box, respectively) are indexed by upper and lower graphs using a suitable ordering of the corresponding Motzkin words, though this is not shown explicitly. Of our examples seen above, 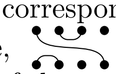, 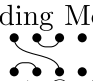 and 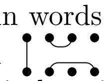 have the same upper graphs and are found in the same column of the rank-1 $\mathscr{D}$-class, in locations $(2, 10), (6, 10)$ and $(11, 10)$ of the 12×12 matrix. Example 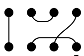 is absent because it is non-planar, and 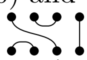 is of rank 2 and not shown. Idempotency and membership in $\mathscr{J}_4$ and $\mathscr{PJ}_4$ are shown by various shadings. Note how distinct $\mathscr{D}$-classes of $\mathscr{PJ}_4$ may have the same rank (so in general a $\mathscr{D}$-class of $\mathscr{M}_n$ may contain multiple $\mathscr{D}$-classes of $\mathscr{PJ}_n$, unlike the situation with $\mathscr{J}_n$).

Now at last we can begin to describe a useful structure on $E(\mathscr{M}_n)$. In what follows, we blur the distinction between α and $\Gamma(\alpha)$, in effect describing elements of $\mathscr{M}_n$ interchangeably by diagrams or interface graphs. (There is confusion possible only when we write of components, because α and $\Gamma(\alpha)$ have different components; this is why we introduced the term Γ-*components*.)

3 A mapping on $E(\mathscr{M}_n)$ and a counting method

Let $\alpha \in E(\mathscr{M}_n)$. Our first definition uses, as foreshadowed, the representation of α as an interface graph. Let α have active vertices $i'_1 < i'_2 \cdots < i'_r$ (upwards) and $j_1 < j_2 \cdots < j_r$ (downwards)—we mean, of course, in $\Gamma(\alpha)$. Note that necessarily these sets are of equal cardinality $r = \mathrm{rank}(\alpha)$.

Figure 2: The lowest two Green's $\mathscr{D}$-classes of the Motzkin monoid $\mathscr{M}_4$, with elements represented by interface graphs. Elements of the Jones monoid $\mathscr{J}_4$ are shaded in green and those of the complement $\mathscr{P}\mathscr{J}_4 \setminus \mathscr{J}_4$ in partial Jones shown in pink; non-idempotents are hatched in grey.

Definition. Let $s = 2\lfloor \frac{r}{2} \rfloor$. If $r = 0$ or 1, we set $\widehat{\alpha} = \alpha$. Otherwise, construct $\widehat{\alpha}$ by adding to α the edges $i'_1 i'_2, i'_3 i'_4, \ldots, i'_{s-1} i'_s$ (above the interface) and $j_1 j_2, j_3 j_4, \ldots, j_{s-1} j_s$ (below the interface).

Examples of this mapping are 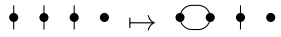 and 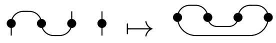. We note that if $\alpha \in \mathscr{P}\mathscr{J}_n$ it may be that $\widehat{\alpha} \notin \mathscr{P}\mathscr{J}_n$; for an example, consider 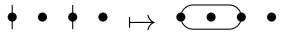. This is the key reason that the method of this section fails for $\mathscr{P}\mathscr{J}_n$.

We collect notable properties of the map $\alpha \mapsto \widehat{\alpha}$ in the next proposition.

Proposition 3.1. Let $\alpha \in E(\mathscr{M}_n)$ and the rank of α have parity $p \in \{0, 1\}$. Then

(i) $\widehat{\alpha} \in E(D_p(\mathscr{M}_n))$;

(ii) the new edges form cycle components of $\widehat{\alpha}$, and all the new components are to the left of any transversal of $\widehat{\alpha}$;

(iii) if $\alpha \in \mathscr{J}_n$ then $\widehat{\alpha} \in D_p(\mathscr{J}_n)$;

(iv) the map $\alpha \mapsto \widehat{\alpha}$ is onto D.

Proof. (i,ii) The new edges may be drawn without intersecting other edges, so $\widehat{\alpha} \in \mathscr{M}_n$ follows from the definitions. The vertices i'_1, j_1 make a transversal edge in the diagram representation of α, and are at level 0 (in representation (iii)); likewise, i'_2, j_2 form a transversal at level 1. Since α is idempotent, the Γ-component containing i'_1 must contain a vertex at the same level active downwards, and this can only be j_1. Similarly for i'_2 and j_2. If we now define $\alpha^{\downarrow}$ to be the element formed by adding to α the edges $i'_1 i'_2$ and $j_1 j_2$, we see that these edges lie in the same Γ-component of $\alpha^{\downarrow}$, which is a cycle. Hence $\alpha^{\downarrow} \in E(\mathscr{M}_n)$ by Proposition (2.1). Moreover this cycle is to the left of the leftmost transversal of $\widehat{\alpha}$. Now $\operatorname{rank}(\alpha^{\downarrow}) = \operatorname{rank}(\alpha) - 2$, so the sequence $\alpha, \alpha^{\downarrow}, \alpha^{\downarrow\downarrow}, \ldots \widehat{\alpha}$ eventually terminates in an element of $E(D_p)$. (iii) No inert vertices are produced in the construction. (iv) $\widehat{\delta} = \delta$ for each $\delta \in D$. ☐

It follows that $E = E(\mathscr{M}_n)$ is partitioned into blocks $F_\delta = \{\alpha \in E \ : \ \widehat{\alpha} = \delta\}$, the $\widehat{\ }$-fibres of $\delta \in D$. We want to count the elements of these blocks, and so we investigate their structure.

3.1 The structure of F_δ

This investigation requires another description of the fibres. Let $\delta \in D$ be fixed.

Definition. For any $\alpha \in \mathscr{M}_n$, let $\Theta(\alpha)$ be the set of cyclic Γ-components of α *to the left of the leftmost transversal* or, for short, LLT.

If there are no transversals, the constraint is of course void, and if $\alpha \in D$, there is at most one transversal. If there is a LT, it is distinguished by having at least one edge at level 0.

Definition. A pair consisting of one upper and one lower return edge from the same cycle Γ-component $\theta \in \Theta(\delta)$ will be called a *special pair* over θ.

Using our convention about dashes, a special pair may be denoted by (e', f), where (say) $e' = i'j'$ and $f = kl$ are respectively lower and upper edges of θ.

Definition. Let $\delta \in D$ and fix $\theta \in \Theta(\delta)$. Suppose $\alpha \in \mathscr{M}_n$ is such that $\theta \in \Theta(\alpha)$, and let (e', f) be a special pair over θ. Let β be formed from α by removing e' and f, and designating all the new terminal vertices as active on the appropriate sides. Then we call β a *θ-cover* of α, and write variously $\alpha \prec_\theta \beta$, $\alpha - \beta = (e', f)$ and $\alpha - (e', f) = \beta$.

The different notations exist for specific purposes—$\alpha \prec_\theta \beta$ may hold for distinct β, but $\beta = \alpha - (e', f)$ defines β uniquely for the given data. Here are a couple of examples. Suppose $\delta =$ ; then the Γ-component on $\{1,2\}$ is the only member of $\Theta(\delta)$, and $(1'2', 12)$ is a special pair over $\theta = \{1,2\}$. So $\delta - (1'2', 12) =$ 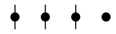 and $\delta \prec_\theta$ 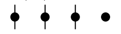 . Again, if $\delta =$ , then the sole Γ-component is δ itself, and both $(3'4', 14)$ and $(1'2', 14)$ are special pairs over δ. Then $\delta -$ 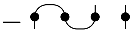 $= (3'4', 14)$, and $\delta \prec_\theta$ , etc. Observe that 23 is not a return edge in 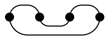 (it is a return at level 1) and so cannot take part in a special pair. Also, it is necessary that return edges are to the left of any transversal in δ: if $\delta =$ , then $(4'5', 45)$ is not a special pair because the edges are at level 1.

Proposition 3.2. Let $\delta \in D$, $\theta \in \Theta(\delta)$, $\alpha, \beta \in \mathscr{M}_n$ and $\alpha \prec_\theta \beta$. Then (i) $\alpha \in E(\mathscr{M}_n)$ implies $\beta \in E(\mathscr{M}_n)$ and (ii) $\alpha \in \mathscr{J}_n$ implies $\beta \in \mathscr{J}_n$.

Proof. (i) By Proposition 2.1, α contains no mixed path and no cis-active path. The Γ-component θ is a cycle by definition, and the removal of a special pair results in the replacement of θ by two trans-active paths. Hence β is idempotent by Proposition 2.1. (ii) Similarly, no inert vertices are introduced when a special pair is removed. □

Definition. Let $\alpha, \beta \in E(\mathscr{M}_n)$. Write $\alpha \ll_\delta \beta$ if $\alpha = \beta$ or there exist distinct $\theta_\iota \in \Theta(\delta)$ (indexed by $\iota = 1, \dots, h$) and idempotents α_ι such that

$$\alpha = \alpha_0 \prec_{\theta_1} \alpha_1 \cdots \prec_{\theta_h} \alpha_h = \beta. \tag{1}$$

We refer to the chain in (1) as a sequence of *mutations* between α and β. Note that (by Proposition 3.2(i)) we need only specify that α is idempotent, rather than all α_ι. The interval $\{\gamma : \alpha \ll_\delta \gamma \ll_\delta \beta\}$ in this order will be denoted $[[\alpha, \beta]]_\delta$ or simply $[[\alpha, \beta]]$ in context. For an example with $n = 5$, take $\delta =$ , with $\theta_1 = \{1,2\}$ and $\theta_2 = \{3,4\}$. Then

$\delta \prec_{\theta_1}$ 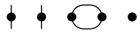 $\prec_{\theta_2}$  ,

and so $\delta \ll_\delta$  . The point of this is in the next proposition.

Proposition 3.3. Let $\delta \in D$ and $\alpha \in E(\mathscr{M}_n)$. Then $\widehat{\alpha} = \delta$ if and only if $\delta \ll_\delta \alpha$.

Proof. Suppose $\widehat{\alpha} = \delta$. Set $h = 2\lfloor \frac{r}{2} \rfloor, \alpha_h = \alpha$, and for $\iota = 1, \dots, h$ let $\alpha_{\iota-1} = \alpha_\iota^\downarrow$ as defined in the proof of Proposition 3.1. As argued in that proof, there is a cycle $\theta_\iota \in \Theta(\delta)$ such that $\alpha_{\iota-1} \prec_\theta \alpha_\iota = \alpha_\iota^2$ for $\iota = 1, \dots, h$ and $\alpha_0 = \delta$. Thus we have

$$\delta = \alpha_0 \prec_{\theta_1} \alpha_1 \cdots \prec_{\theta_h} \alpha_h = \alpha. \tag{2}$$

Conversely, suppose (2) holds, and that $\widehat{\alpha_{\iota-1}} = \delta$ (as is true for $\iota = 1$). Then $\mathrm{rank}(\alpha_{\iota-1}) = \mathrm{rank}(\delta) + 2(\iota - 1)$ and there are active vertices $i_1 < \cdots < i_{2(\iota-1)}$ (downwards) and $j'_1 < \cdots < j'_{2(\iota-1)}$ (upwards) in $\alpha_{\iota-1}$, and moreover a special pair (e', f) in some $\theta \in \Theta(\delta)$ such that $\alpha_{\iota-1} - \alpha_\iota = (e', f)$. Suppose first that δ has rank 1, with transversal $i_* j'_*$. Then $i_1 j'_1, \dots, i_{2(\iota-1)} j'_{2(\iota-1)}, i_* j'_*$ is the complete list of transversals of $\alpha_{\iota-1}$, and (e', f) lies to the left of $i_1 j'_1$ or between two transversals of this list. It follows that $\widehat{\alpha_\iota} = \widehat{\alpha_{\iota-1}} = \delta$. The case of $\mathrm{rank}(\delta) = 0$ reaches the same conclusion in like manner. □

If there is such a chain (2), we say that each special pair $\alpha_{\iota-1} - \alpha_\iota = \{e_\iota, f_\iota\}$ *occurs in the interval* $[[\delta, \alpha]]$ from δ to α. This is meaningful, because the order of the special pairs in (2) is irrelevant: the above proof also shows that if $\widehat{\alpha} = \delta$ as in (2) above, and π is any permutation of $\{1, \dots, h\}$, then there exist β_ι such that $\beta_{\iota-1} - \beta_\iota = \{e'_{\iota\pi}, f_{\iota\pi}\}$, and (1) of the definition applies. We may observe this in the previous example, where there is another chain with a different interior member,

$\delta \prec_{\theta_2}$ 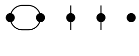 $\prec_{\theta_1}$ 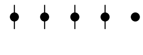 .

3.2 Counting the idempotents

Now we come to our counting method. A couple of notational definitions are convenient at this point.

Definition. For $\delta \in D$ and $\theta \in \Theta(\delta)$, let $C^*_\delta(\theta)$ be the set of θ-covers of δ and $C_\delta(\theta) = C^*_\delta(\theta) \cup \{\delta\}$. Let u_θ, l_θ be the numbers of upper and lower returns respectively in θ.

Immediately from this definition we have

Lemma 3.4. $|C^*_\delta(\theta)| = u_\theta l_\theta$.

The following proposition applies to both $\mathscr{J}_n$ and $\mathscr{M}_n$.

Proposition 3.5. F_δ is bijective with the product of subsets $C_\delta(\theta)$ as θ runs through the set $\Theta(\delta)$ of cyclic Γ-components of δ LLT, that is,

$$F_\delta \cong \prod\{C_\delta(\theta) : \theta \in \Theta(\delta)\}. \tag{3}$$

Proof. We want to define a map of F_δ to $\prod\{C_\delta(\theta) : \theta \in \Theta(\delta)\}$. So, for each $\theta \in \Theta(\delta)$ and $\alpha \in F_\delta$, the assignment

$$f_\theta : \alpha \mapsto \begin{cases} \delta - (e', f), & \text{if } \ e', f \text{ are edges of } \theta \text{ and } (e', f) \text{ occurs in } [[\delta, \alpha]]_\delta, \\ \delta, & \text{otherwise,} \end{cases} \tag{4}$$

is well-defined, since if (e'_1, f_1) and (e'_2, f_2) both occur in $[[\delta, \alpha]]$, they belong to different components θ_1 and θ_2. Clearly, $f_\theta : F_\delta \to C_\delta(\theta)$ since $\delta - (e', f)$ in (4) covers δ. So the f_θ all factor through the product $\prod\{C_\delta(\theta) : \theta \in \Theta(\delta)\}$ and there is $f : F_\delta \to \prod\{C_\delta(\theta) : \theta \in \Theta(\delta)\}$ such that $f_\theta = f \circ \mathrm{pr}_\theta$. Now if $\alpha f = \beta f$, then $\alpha f_\theta = \beta f_\theta$ for all $\theta \in \Theta(\delta)$, which is to say that there are chains in the intervals $[[\delta, \alpha]]$ and $[[\delta, \beta]]$ in which the same edge-pairs occur. Thus $\alpha = \beta$, and we conclude that f is injective. There is also a function $g : \prod\{C_\delta(\theta) : \theta \in \Theta(\delta)\} \to F_\delta$ under which a sequence of edges in the product are removed from δ to give $\alpha \in F_\delta$; f and g are inverses. □

We may summarise this line of reasoning in a theorem which provides the foundation for our results.

Theorem 3.6. Let S be $\mathscr{M}_n$ or $\mathscr{J}_n$. Then $E(S)$ is the disjoint union of the set of F_δ as δ ranges over $D(S)$, and thus

$$|E(S)| = \sum_{\delta \in D(S)} f_\delta, \text{ where } f_\delta = \prod_{\theta \in \Theta(\delta)} (1 + u_\theta l_\theta). \quad \square$$

Note that the product expression for f_δ may be taken over only those $\theta \in \Theta(\delta)$ such that $u_\theta l_\theta \neq 0$ (equivalently such that θ has at least one upper and one lower return).

Remark. We saw above that the map $\widehat{\cdot}$ does not preserve membership of $\mathscr{P}\mathscr{J}_n$. However, the mutation process (upwards) does, and so when $S = \mathscr{P}\mathscr{J}_n$, the method of Theorem 3.6 gives only a lower bound: $|E(\mathscr{P}\mathscr{J}_n)| \geq \sum\{f_\delta : \delta \in D(\mathscr{P}\mathscr{J}_n)\}$. Theorem 3.6 also permits the counting of the idempotents of the planar part $\pi\mathscr{P}_n$ of the partition monoid, since $\pi\mathscr{P}_n \cong \mathscr{J}_{2n}$ [7].

Let us apply the method to a previous example. Let $\delta =$ $\in D(\mathscr{M}_8)$. From Table 1 (or inspection) we see $u_\theta = 1 = l_\theta$, so $f_\delta = 2$. The idempotent covering δ is

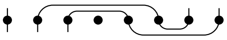 and the fibre F_δ consists of just these two elements. Now (a minor modification of a previous example) let

$$\delta =$$ 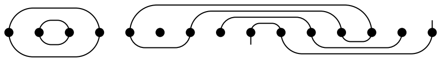 $$\in D(\mathscr{M}_{15}).$$

There are two cycles having both upper and lower returns, namely those on vertex sets $\{1, 4\}$ and $\{5, 7, 12, 13\}$. In each case $1 + u_\theta l_\theta = 2$, so $f_\delta = 2 \times 2 = 4$. The two idempotent covers of δ are 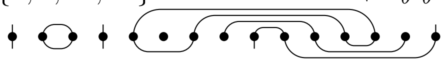 and 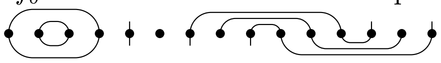 .

The main advantage of this method over the generation and testing of all members of $S \subseteq \mathscr{P}_n$ is that it requires a vanishingly small fraction of elements to be processed. In the case of $\mathscr{J}_n$, this can be illustrated by using the asymptotic estimate in A000108 of OEIS [20], $C_n \sim \frac{4^n}{\sqrt{\pi n}(n+1)}$. We shall see, in Corollary 6.2, that $|D| = C^2_{\lceil \frac{n}{2} \rceil}$. Then we have, for even n, $\frac{|D|}{|\mathscr{J}_n|} \sim \frac{2(n+1)4}{\sqrt{\pi n}(n+2)^2} \sim \frac{8}{\sqrt{\pi n}(n+3)}$ and, for n odd, $\frac{|D|}{|\mathscr{J}_n|} \sim \frac{2\sqrt{n}.4.4}{\sqrt{\pi}(n+3)^2} \sim \frac{32\sqrt{\frac{n}{\pi}}}{(n+3)^2}$. In each case the ratio is $O(n^{-\frac{3}{2}})$.

3.3 Enumeration by rank

For a vector $\mathbf{x} = (x_i)_{i \in I}$, write

$$f(\mathbf{x}) = \prod_{i \in I}(1 + x_i) = 1 + \sum x_i + \sum_{i \neq j} x_i x_j + \cdots + \prod x_i \tag{5}$$

$$= 1 + \sigma_1(\mathbf{x}) + \sigma_2(\mathbf{x}) + \cdots + \sigma_{|I|}(\mathbf{x}), \tag{6}$$

where σ_d is the elementary symmetric form of degree d. By convention, $\sigma_0(\mathbf{x}) = 1$ and $\sigma_d(\mathbf{x}) = 0$ if $d > |I|$. For $\delta \in D$, write $\mathbf{x}_\delta = (u_\theta l_\theta)_{\theta \in \Theta(\delta)}$. Then $f_\delta = |F_\delta| = f(\mathbf{x}_\delta)$, and (6) may be thought of as an enumeration of F_δ by ranks. Indeed, in the chain (2), $\operatorname{rank}(\alpha_\iota) = 2\iota + \operatorname{rank}(\delta)$ for all $\iota = 0, \ldots, h$; thus, if $0 \leq r = 2k + p \leq n$, where $k \in \mathbb{Z}$ and $p \in \{0, 1\}$, then the set $\{\alpha \in E(S) \colon \operatorname{rank}(\alpha) = r\}$ has size

$$\sum_{\delta \in E(D_p)} \sigma_k(\mathbf{x}_\delta).$$

3.4 Geometry of $E(\mathscr{M}_n)$

The development above is entirely set-theoretic, but a geometric interpretation is also of interest. Let $\delta \in D$, and $\theta \in \Theta(\delta)$. Each $C(\theta)$ is a fan—a pointed complex of 1-cells, $u_\theta l_\theta$ in number—over the base point δ. Then F_δ is a pointed product, over the base point, of the $C(\theta)$, and so its k-cells are indexed by k-sets from the special pairs available in δ. Those components of $\Theta(\delta)$ lacking either top or bottom return edges contribute only the trivial pointed complex, and so do not change the product. Figure 2 shows a small part of the structure of $E(\mathscr{M}_7)$—just three fibres (out of 25 171).

4 Idempotents of the twisted Jones and Motzkin monoids

Given a semigroup S and a field $\Bbbk$, the *semigroup algebra* $\Bbbk[S]$ is defined as the set of functions $\phi \colon S \to \Bbbk$ having finite support. It is traditional to write ϕ as $\sum_{s \in S} a_s s$, where $a_s = s\phi$, and only terms with non-zero coefficients need be written down. Addition is defined pointwise, and multiplication extended from S by distributivity. As a vector space, it has a defining basis S.

A map $\tau : S \times S \to \Bbbk^\times = \Bbbk \setminus \{0\}$ is a *twisting* if (written exponentially) it satisfies

$$(a, b)^\tau (ab, c)^\tau = (a, bc)^\tau (b, c)^\tau$$

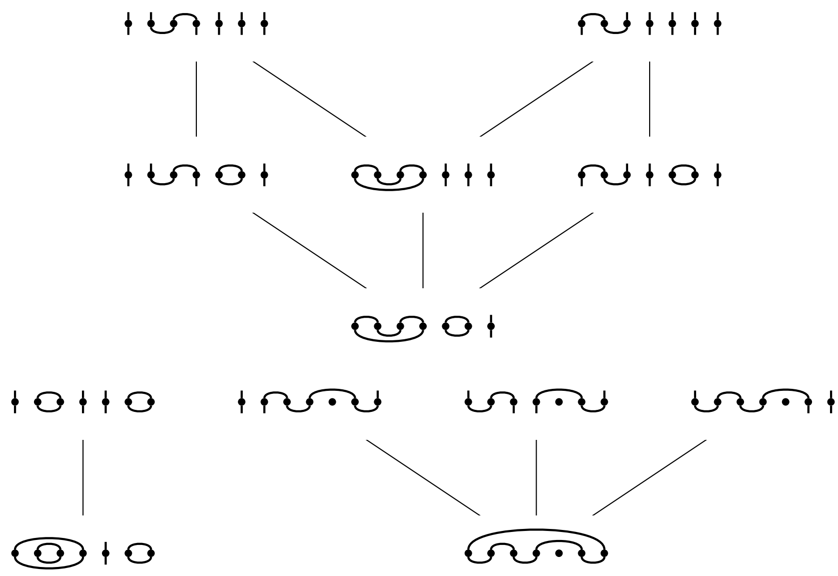

Figure 3: Three fibres of $\big(E(\mathscr{M}_7), \ll\big)$ shown as Hasse diagrams or cell complexes.

for all $a, b, c \in S$, which is equivalent to associativity of the altered or twisted multiplication on the defining basis elements of $\Bbbk[S]$ given by

$$a \circ b = (a, b)^\tau ab.$$

This multiplication, extended by distributivity to the elements of $\Bbbk[S]$, results in the *twisted semigroup algebra* $\Bbbk^\tau[S]$. The case in which $\tau(\alpha, \beta) \equiv 1$ is simply the original 'plain' semigroup algebra $\Bbbk[S]$. Let us define a semigroup S^τ to be the subsemigroup of $\Bbbk^\tau[S]$ generated by S, so that the twisted semigroup algebra $\Bbbk^\tau[S]$ is identical to the plain semigroup algebra $\Bbbk[S^\tau]$. (The advantage of $\Bbbk^\tau[S]$ is that $\Bbbk^\tau[S]$ has the same dimension as $\Bbbk[S]$, namely $|S|$, while $\Bbbk[S^\tau]$ may be infinite-dimensional even when S is finite.) The semigroup S^τ is called the *twisted* variant of S. The elements of S^τ are all of the form $k\alpha$ for some scalar k and $\alpha \in S$, but which scalars are actually used in S^τ depends on the specific twisting. If S_1, S_2 are subsemigroups of S, it is clear that $S_1 \subseteq S_2$ implies $S_1^\tau \subseteq S_2^\tau$.

A 'natural' twisting is available for $\mathscr{P}_n$, and hence for any of its subsemigroups S. Let $\alpha, \beta \in \mathscr{P}_n$ and let $m(\alpha, \beta)$ be the number of components formed in the product graph $\Gamma(\alpha, \beta)$ which have vertex sets contained entirely within the interface, as described in Section 2 of [4]. (Remember we call such a component *floating*.) It is readily verified that $m(\alpha, \beta) + m(\alpha\beta, \gamma) = m(\alpha, \beta\gamma) + m(\beta, \gamma)$. Now fix a $\xi \in \Bbbk^\times$; this property of m shows that the definition

$$(\alpha, \beta)^\tau = \xi^{m(\alpha,\beta)}$$

gives a twisting. (We consider the case of $\xi = 0$ later.)

In geometric terms, what happens is that the 'plain' product acquires an extra factor of ξ for each floating component that forms in the interface of the graph $\alpha + \beta$ described in Section 2 above. The resulting twisted variant of S is denoted by S^ξ and each of its elements has the form $\xi^i \alpha$ for some $i \in \mathbb{N}$ and $\alpha \in S$. The multiplication in S^ξ is

$$\xi^i \alpha \circ \xi^j \beta = \xi^{i+j+m(\alpha,\beta)} \alpha\beta. \tag{7}$$

Again, if $\xi = 1$ we have exactly the 'plain' S. Our aim in this section is to enumerate idempotents in the twisted Jones monoids. Of course, these are not coextensive with idempotents of the twisted algebras, since there are non-trivial linear combinations which are multiplicative idempotents, such as $\frac{1}{2}(e+f)$ where $e \mathscr{L} f$ (that is, $ef = e$ and $fe = f$). We continue by deducing the form of idempotents in S^ξ.

Lemma 4.1. The element $\xi^i\alpha \in S^\xi$ is an idempotent if and only if $\xi^{i+m(\alpha,\alpha)} = 1$ and α is an idempotent in S.

Proof. By equation (7), $\xi^i\alpha \circ \xi^i\alpha = \xi^i\alpha$ if and only if $\xi^{2i+m(\alpha,\alpha)}\alpha^2 = \xi^i\alpha$ or equivalently, by the definition of equality in the semigroup algebra, $\alpha^2 = \alpha$ and $\xi^{i+m(\alpha,\alpha)} = 1$. □

This is not yet a characterisation of idempotents, as we do not know for which $i \in \mathbb{N}$ we have $\xi^i\alpha \in S^\xi$. So for the remainder of this section, let S be either of $\mathscr{M}_n$ or $\mathscr{J}_n$, as we can be much more specific in these cases.

Lemma 4.2. If $\alpha \in S \setminus \{1\}$ then $\xi\alpha \in S^\xi$.

Proof. First take $S = \mathscr{J}_n$ and let h_i be the initial letter in the Jones normal form for α. Then since $h_i^2 = h_i$, $\alpha = h_i\alpha$ in $\mathscr{J}_n$, while $h_i \circ \alpha = \xi\alpha$ in $\mathscr{J}_n^\xi$. Next take $S = \mathscr{M}_n$. By the *PTP* form of Hatch et al. [8], $\mathscr{M}_n$ is generated by Jones elements h_i and planar rook monoid generators l_i, r_i, which are partial bijections with domains $X \setminus \{i+1\}$ and $X \setminus \{i\}$ respectively. If h_i is the first letter in the normal form for α, the argument goes exactly as for $\mathscr{J}_n$. If l_i is the first letter, let e_{i+1} be the partial identity on domain $X \setminus \{i+1\}$, so that $e_{i+1} \in \mathscr{M}_n$ and $e_{i+1}\alpha = \alpha$ in $\mathscr{M}_n$, while $e_{i+1} \circ \alpha = \xi\alpha$ in $\mathscr{M}_n^\xi$. Finally if r_i is the first letter, the argument is similar. □

Corollary 4.3. $S^\xi = \{1, \xi^i\alpha : i \in \mathbb{N}, \alpha \in S \setminus \{1\}\}$.

Proof. From Lemma 4.2, $S \subseteq \mathrm{RHS} \subseteq S^\xi$; but RHS is a subsemigroup. □

We study S^ξ with the aid of two monoids within which it is contained, namely $\langle S^\xi, \xi 1\rangle = \{\xi^i\alpha : i \in \mathbb{N},\ \alpha \in S\}$ and $\langle S^\xi, \xi 1, \xi^{-1}1\rangle = \{\xi^i\alpha : i \in \mathbb{Z},\ \alpha \in S\}$.

The structures of these semigroups depend on whether $\xi^{-1} \in \langle\xi\rangle$, and so we must consider two cases: the *periodic* case where $\xi^i = 1$ for some $i \in \mathbb{N}$ and $\xi^{-1} \in \langle\xi\rangle$, and the *generic case* where ξ is not a root of unity and all three semigroups are distinct. We can now characterise idempotents in these semigroups.

Proposition 4.4. (i) There is a bijection between $E(S)$ and $E(\langle S^\xi, \xi 1, \xi^{-1}1\rangle)$, in which $\alpha \in E(S)$ if and only if $\xi^{-m(\alpha,\alpha)}\alpha \in E(\langle S^\xi, \xi 1, \xi^{-1}1\rangle)$;
(ii) if ξ is a root of unity, $|E(\langle S^\xi, \xi 1\rangle)| = |E(S)|$; and
(iii) in the generic case, $E(\langle S^\xi, \xi 1\rangle) = E(S^\xi) = \{\alpha \in E(S) : m(\alpha,\alpha) = 0\}$.

Proof. Part (i) follows from Lemma 4.1. If ξ is a root of unity, $\xi^{-1} \in \langle\xi\rangle$ and part (i) applies. In the generic case, Lemma 4.1 implies $\xi^i\alpha \in E(S^\xi)$ if and only if $\alpha \in E(S)$ and $i = m(\alpha,\alpha) = 0$. □

The only new interest is therefore in the generic case. Even this turns out to be the same for our two choices of S:

Lemma 4.5. Suppose ξ is not a root of unity. Then $E(\mathscr{M}_n^\xi) = E(\mathscr{J}_n^\xi)$.

Proof. Clearly $E(\mathscr{J}_n^\xi) \subseteq E(\mathscr{M}_n^\xi)$. But if $\xi^i\alpha \in E(\mathscr{M}_n^\xi)$, then by Proposition 4.4 (iii), $\alpha \in E(\mathscr{M}_n)$ and $m(\alpha,\alpha) = 0$. In particular, there can be no inert vertices in the interface graph of α, so that $\alpha \in \mathscr{J}_n$ and equality of the sets follows. □

Kauffman [14] gave a presentation of $\mathscr{J}_n^\xi$ based on that for the Jones monoid, and the generic case is now called the *Kauffman monoid* [2]. We may modify the formulæ of Theorem 3.6 to compute $|E(\mathscr{J}_n^\xi)|$, and hence of $|E(\mathscr{M}_n^\xi)|$, both of which we denote by e_n^ξ. We use RLT to mean *to the right of the leftmost transversal*.

Proposition 4.6. The cardinality of $E(\mathscr{J}_n^\xi)$ is given by $\sum\{b_\delta^\xi : \delta \in D\}$, where

$$b_\delta^\xi = \begin{cases} 0, & \text{if } \delta \text{ has a cycle RLT}, \\ 1, & \text{if } \delta \text{ is a path}, \\ \prod\{u_\theta l_\theta : \theta \in \Theta(\delta)\}, & \text{otherwise.} \end{cases}$$

Proof. Each cycle-free $\alpha \in E(\mathscr{J}_n)$ is maximal in its block F_δ and there are $\prod\{u_\theta l_\theta : \theta \in \Theta(\delta)\}$ maximal elements. Let B_δ^ξ be the set of maximal elements in F_δ which are free of cycles, and b_δ^ξ its cardinality. Now $B_\delta^\xi = \emptyset$ if δ has a cycle RLT, or a cycle θ LLT with every upper or every lower edge a non-return. (In the latter case, $u_\theta l_\theta = 0$.) Also, $B_\delta^\xi = \{\delta\}$ if δ has exactly one path and no cycles. Since $E(\mathscr{J}_n^\xi) = \bigcup\{B_\delta^\xi : \delta \in D\}$ we have the result. □

Finally we consider the case $\xi = 0$, omitted by definition at the beginning of this section. Equation (7) becomes

$$\alpha \circ \beta = \begin{cases} \alpha\beta, & \text{if } m(\alpha, \beta) = 0, \\ 0, & \text{otherwise,} \end{cases} \tag{8}$$

resulting in a semigroup $S^{\xi=0} = (S \cup \{0\}, \circ)$. In this semigroup, $\alpha \in E(S^{\xi=0})$ if and only if $\alpha = 0$ or $\alpha \in E(S^\xi)$, and so $|E(\mathscr{M}_n^{\xi=0})| = |E(\mathscr{J}_n^{\xi=0})| = e_n^\xi + 1$.

The results from this section may be compared with Section 6 and Theorem 33 of [4].

5 Tabulated values

Table 2 presents computed values, denoted e_n, of the idempotent numbers in $\mathscr{M}_n$ for $0 \le n \le 8$, both in total and as stratified by rank. The Motzkin idempotent numbers now appear in the OEIS [20] as sequence A256672. Recall from Section 2.1 that the values of $|\mathscr{M}_n|$ in Table 2 are

Table 2: Values of idempotent numbers in $\mathscr{M}_n$ by rank r, with total idempotents e_n, total elements $|\mathscr{M}_n|$, and fraction of idempotents $e_n/|\mathscr{M}_n|$ to 3 d.p., $n \le 8$.

$r \backslash n$	0	1	2	3	4	5	6	7	8
0	1	1	4	16	81	441	2601	16 129	104 329
1		1	2	11	48	266	1492	9042	56 712
2			1	3	19	93	549	3211	20 004
3				1	4	28	152	947	5784
4					1	5	38	226	1480
5						1	6	49	316
6							1	7	61
7								1	8
8									1
e_n	1	2	7	31	153	834	4839	29 612	188 695
$\|\mathscr{M}_n\|$	1	2	9	51	323	2188	15 511	113 634	853 467
$e_n/\|\mathscr{M}_n\|$	1	1	.778	.608	.474	.381	.312	.261	.221

the *even Motzkin numbers*, appearing in [20] as sequence A026945. The squares of the Motzkin sequence (A001006 of [20]) make up row $r = 0$ of Table 2. It can be seen that in all cases calculated, more than half of the idempotents in $\mathscr{M}_n$ have rank 0. Let us fix $d \in \mathbb{N}$ and define the d-th diagonal of Table 2 as the sequence of entries with $r = n - d$. Then it may be observed empirically that the d-th difference in the d-th diagonal is equal to 1. We hope to study this phenomenon in another place.

Table 3 presents computed values, for $1 \le n \le 9$, of the idempotent numbers in $\mathscr{J}_n$, stratified by rank. The many blanks above the diagonal in Table 3 reflect a parity constraint, which may be obviated by using an alternative parametrisation of the $\mathscr{D}$-classes. Again, $|E(\mathscr{J}_n)|$ is denoted e_n. All elements of $\mathscr{J}_n$ have $n-r$ even, so that the *depth* $d = \frac{n-r}{2}$ is an integer in $0 \le d \le \lfloor \frac{n}{2} \rfloor$. Table 4 gives $|E(\mathscr{J}_n)|$ at different depths d. Somewhat as in Table 2, there are patterns in the differences which may be observed, and these are discussed further in Section 6.

Table 3: Values of idempotent numbers in $\mathscr{J}_n$ by rank r, with total idempotents e_n and total elements $|\mathscr{J}_n|$, $n \le 9$.

$r\backslash n$	0	1	2	3	4	5	6	7	8	9
0	1		1		4		25		196	
1		1		4		25		196		1764
2			1		7		57		522	
3				1		10		98		1006
4					1		13		148	
5						1		16		207
6							1		19	
7								1		22
8									1	
9										1
e_n	1	1	2	5	12	36	96	311	886	3000
$\lvert\mathscr{J}_n\rvert$	1	1	2	5	14	42	132	429	1430	4862

Table 4: Values of idempotent numbers in $\mathscr{J}_n$ ($1 \le n \le 12$) by depth d (instead of rank as above), with totals e_n, fraction of idempotents e_n/C_n, maximum fraction of idempotents with equal rank (both to 3 d.p.), and Kauffman idempotent numbers e_n^{ξ}.

$d\backslash n$	1	2	3	4	5	6	7	8	9	10	11	12
0	1	1	1	1	1	1	1	1	1	1	1	1
1		1	4	7	10	13	16	19	22	25	28	31
2				4	25	57	98	148	207	275	352	438
3						25	196	522	1006	1673	2550	3664
4								196	1764	5206	10 837	19 261
5										1764	17 424	55 319
6												17 424
e_n	1	2	5	12	36	96	311	886	3000	8944	31 192	96 138
e_n/C_n	1	1	.857	.857	.727	.725	.620	.617	.533	.531	.462	.461
d_n^*/e_n	1	.5	.8	.583	.694	.594	.630	.589	.588	.582	.559	.575
e_n^{ξ}	1	1	3	5	15	31						

Table 4 also presents the totals e_n for each n, and the idempotent number as a fraction of the size C_n of $\mathscr{J}_n$. The Jones idempotent numbers appear in the OEIS [20] as sequence A225798. It is perhaps noteworthy that over one-half of the Jones idempotents occur in one $\mathscr{D}$-class (of rank 1 or 2 depending on parity of n) out to $n = 12$, which is all the by-ranks data we currently have. This size of the maximum contribution from a single $\mathscr{D}$-class is denoted d_n^*, and the sequence of fractions d_n^*/e_n is also given in Table 4. This sequence has decreasing first differences which alternate in sign frequently but not regularly. Thus Table 4 suggests that the following conjectures are not far-fetched.

Conjectures 5.1. (i) For each $n > 1$, $d_n^* = \max_r |\{\alpha \in E_n \colon \operatorname{rank}(\alpha) = r\}|$ occurs at $r = 1$ when n is odd, and at $r = 2$ when n is even;
(ii) for $n \ge 4$, $2d_n^* > e_n$.

Conjecture 5.1(i), if true, leads to bounds $d_n^* < e_n < 2d_n^*$. We return to this matter in the next section, in a Remark after Corollary 6.2.

In Table 5 the sequence e_n of Table 4 is extended to cases $13 \le n \le 24$. The values in Tables 2–5 have been checked by other methods wherever feasible, principally by exhaustive enumeration

Table 5: Values of idempotent numbers in $\mathscr{J}_n, 13 \le n \le 24$, with fraction of idempotents e_n/C_n.

n	13	14	15	16	17	18
e_n	342 562	1083 028	3923 351	12 656 024	46 455 770	152 325 850
e_n/C_n	.461	.405	.405	.358	.358	.319
n	19	20	21	22	23	24
e_n	565 212 506	1878 551 444	7033 866 580	23 645 970 022	89 222 991 344	302 879 546 290
e_n/C_n	.320	.286	.287	.258	.260	.235

and checking for idempotency using the `Semigroups` package for `GAP` [6, 19]. The idempotent counts for $\mathscr{P}\mathscr{J}_n, 1 \le n \le 10$ are known to be 2, 7, 24, 103, 416, 1998, 8822, 45 661, 213 674, 1167 797 (this is sequence A256492 of [20]). The corresponding lower bounds by the method of Theorem 3.6 are 2, 7, 21, 98, ...

Tables 6 and 7 show sample computation times on a desktop machine for three methods used to compute the sequences e_n for the Motzkin and Jones idempotents. Method 1 is a 'high level' application of GAP, and ran out of memory at $n = 10$. Method 2 (dubbed 'brute force memoryless') checks element-wise and accumulates. Method 3 is the method of Theorem 3.6, again implemented in GAP. The algorithms are discussed further in the Appendix.

Table 6: Comparative run times (in milliseconds) of three methods for computing $e_n = |E(\mathscr{M}_n)|$ for $1 \le n \le 9$.

n	1	2	3	4	5	6	7	8	9
Method 1	10	7	3	7	54	224	1287	9590	84 331
Method 2	2	6	19	101	850	7456	66 813	708 507	5663 081
Method 3	0	0	1	2	13	76	399	2456	16 594

Table 7: Comparative run times (in milliseconds) of two methods for computing $e_n = |E(\mathscr{J}_n)|$ for $1 \le n \le 15$.

n	1	2	3	4	5	6	7	8	9	10	11	12	13	14	15
Method 1	8	6	3	2	3	7	18	67	179	523	1904	6383	27 124	79 611	368 331
Method 2	4	14	3	5	11	53	131	573	1807	8609	29 036	136 907	489 933	3227 569	9597 556

This small experiment provides further evidence for the efficiency of the method developed in this paper. The relative efficiency gains are perhaps greater in the Jones case, especially for even n, since more than half of the idempotents in $\mathscr{M}_n$ must be scanned and they lie in two $\mathscr{D}$-classes (though of course this is still a small fraction of the total elements). The remainder of the paper is focused on the Jones idempotents, although it is clear that the Motzkin monoids also require further study, perhaps along the lines of the following section. We hope to carry out this study in a further article.

6 More on Jones values, including recurrence relations

In this section we specialise to the Jones monoids. Let $E_{n;c,p}$ be the set of idempotents of $\mathscr{J}_n$ having c cycles and p paths (necessarily all trans-active because of idempotency and so of even length), and let $e_{n;c,p} = |E_{n;c,p}|$. Here, p is the rank of the idempotent. Conventionally we set $e_{0;0,0} = 1$. Note that if $E_{n;c,p}$ is non-empty, n, c, p must satisfy $2c + p \le n$, or $c \le \frac{1}{2}(n - p)$, and $n \equiv p (\text{mod } 2)$.

Consider an element $\alpha \in E_{n;c,p}$ and focus on the vertex 1 and the component of the interface graph containing 1. The two main cases to be considered are when 1 is a member of (I) a cycle, and (II) a path.

Case (I): delete vertex 1 and thus leave an even path π. After re-labelling the vertices $2, \dots n$ to $1, \dots n-1$, as we assume throughout, this gives us an element $\tilde{\alpha}$ of $E_{n-1;c-1,p+1}$. The path π is automatically distinguished by being the leftmost in $\tilde{\alpha}$, and so we have a mapping defined by $\alpha \mapsto (\tilde{\alpha}, \pi)$. An example:

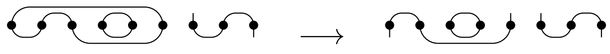

Case (II) has several sub-cases.

Case (IIA): Vertex 1 lies in a singleton component (that is, $\{1, 1'\}$ is the leftmost transversal in the diagrammatic representation). Here we simply delete vertex 1 and obtain $\tilde{\alpha} \in E_{n-1;c,p-1}$. Example:

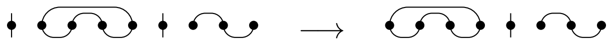

We turn to the cases of paths of positive length.

Case (IIB): 1 is the upward-facing terminus of its path. If we delete 1 and redirect the loosened end around to join the other (downward-facing) terminus, forming a cycle, we obtain $\tilde{\alpha} \in E_{n-1;c+1,p-1}$ possessing a new lower return ρ_L to the left of the leftmost transversal (LLT); write $\alpha \mapsto (\tilde{\alpha}, \rho_L)$. Example:

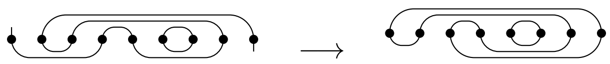

Case (IIC): This is the dual of (B).

Case (IID): 1 is an interior vertex of its path component. Here we delete vertex 1, thus forming two paths, necessarily odd because of planarity, each of which we complete to a cycle by joining the two loose ends. These completed edges (ρ_U and ρ_L, say) are newly created return edges, one upper and one lower, belonging to different cycles, and both LLT. Hence we have a map $\alpha \mapsto (\tilde{\alpha}, \rho_U, \rho_L)$ where $\tilde{\alpha} \in E_{n-1;c+2,p-1}$. Example:

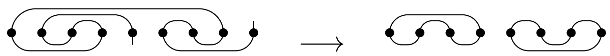

The cases and sub-cases ((I) and (II A–D) listed above above imply a partitioning of $E_{n;c,p}$, and the disjoint union of the respective maps there described gives a map

$$\Phi : E_{n;c,p} \to \{(\tilde{\alpha}, \pi), \tilde{\alpha}, (\tilde{\alpha}, \rho_L), (\tilde{\alpha}, \rho_U), (\tilde{\alpha}, \rho_U, \rho_L)\}. \tag{9}$$

On each of the five parts of the right-hand set in (9), we can easily construct a map back to $E_{n;c,p}$ which has Φ as a left inverse. Specifically, we re-number vertices $1, \dots n-1$ to $2, \dots n$, add the extra vertex 1 and, respectively:

Case (I): close the leftmost path π to a cycle containing 1,

Case (IIA): leave 1 as a singleton component,

Case (IIB): sever the distinguished ρ_L (a lower return LLT) and join its left-hand strand to 1, forming a new path,

Case (IIC): sever the distinguished ρ_U (an upper return LLT) and join its left-hand strand to 1, forming a new path,

Case (IID) : sever the distinguished ρ_U and ρ_L (upper and lower returns from distinct components LLT) and join their left-hand strands to 1, forming a new path.

It follows that Φ in equation (9) is a bijection. Recalling $\Theta(\alpha)$ introduced in Section 3.1, let us define

$$S^{(1)}_{n;c,p} = \sum\{u_\theta + l_\theta \colon \theta \in \Theta(\alpha),\ \alpha \in E_{n;c,p}\},$$
$$S^{(2)}_{n;c,p} = \sum\{u_{\theta_1} l_{\theta_2} \colon \theta_1 \neq \theta_2 \in \Theta(\alpha),\ \alpha \in E_{n;c,p}\}.$$

Then $S^{(1)}_{n-1;c+1,p-1}$ counts the ordered pairs of the forms $(\tilde{\alpha}, \rho_L)$ and $(\tilde{\alpha}, \rho_U)$ in equation (9), and $S^{(2)}_{n-1;c+2,p-1}$ counts the ordered triples $(\tilde{\alpha}, \rho_U, \rho_L)$. Thus we have, from this construction, the following result.

Proposition 6.1. For $n \geq 1$ we have

$$e_{n;c,p} = e_{n-1;c-1,p+1} + e_{n-1;c,p-1} + S^{(1)}_{n-1;c+1,p-1} + S^{(2)}_{n-1;c+2,p-1}.$$

□

If we represent summation over c by using a dot in the corresponding place, note that 'out-of-range' values give zero sums, and abbreviate $S^{(1)} + S^{(2)}$ by $S^{(1+2)}$, we also have

$$e_{n;\,\cdot,p} = e_{n-1;\,\cdot,p+1} + e_{n-1;\,\cdot,p-1} + S^{(1+2)}_{n-1;\,\cdot,p-1}. \tag{10}$$

Corollary 6.2. For all $k \geq 1$,
(i) $e_{2k;\,\cdot,0} = C_k^2 = e_{2k-1;\,\cdot,1}$, where as before C_k is the k-th Catalan number, and
(ii) $e_{2k;\,\cdot,2} = e_{2k+1;\,\cdot,1} - e_{2k;\,\cdot,0} - S^{(1+2)}_{2k;\,\cdot,0}$.

Proof. (i) Since p is the rank, and all elements of minimum rank are idempotents, we know from Section 2 that $e_{2k;\,\cdot,0} = C_k^2$, and then from (10) that $e_{2k;\,\cdot,0} = e_{2k-1;\,\cdot,1} + 0 + 0 + 0$. Part (ii) follows from (10) by setting $n = 2k+1, p = 1$ and rearranging. □

Remark. If Conjecture 5.1 is valid, we have the following bounds on e_n. When $n = 2k+1$,

$$d_n^* = e_{2k+1;\,\cdot,1} = C_{k+1}^2 < e_{2k+1} < 2C_{k+1}^2.$$

When $n = 2k$,

$$C_k^2 < d_n^* = e_{2k;\,\cdot,2} < e_{2k+1;\,\cdot,1} - e_{2k;\,\cdot,0} = C_{k+1}^2 - C_k^2,$$

the second inequality coming from Corollary 6.2 (ii). Thus

$$C_k^2 < e_{2k} < 2(C_{k+1}^2 - C_k^2).$$

These bounds are more extravagant than for the case of n odd. Using $C_n \sim \frac{4^n}{\sqrt{\pi n}(n+1)}$ (A000108 of OEIS [20]) and a little algebra, one sees

$$C_{k+1}^2 - C_k^2 \sim \frac{15.4^{2k}}{\pi k(k+1)^2}.$$

Thus Conjecture 5.1 implies $e_n \sim O(\frac{4^n}{n^3})$. □

There are further interesting connections to these numbers $e_{n;c,p}$. For one, the open and closed *meandric numbers* considered for example in sequence A005316 of [20] (and see also Legendre [17]) are contained in these numbers, as evidently $m_{2k} := e_{2k;1,0}$ and $m_{2k+1} := e_{2k+1;0,1}$. Applying Proposition 6.1 we see

$$\begin{aligned} m_{2k} &= e_{2k;1,0} = e_{2k-1;0,1} + \text{empty sums} = e_{2k-1;0,1} = m_{2k-1}, \\ m_{2k+1} &= e_{2k+1;0,1} = 0 + S^{(1)}_{2k;1,0} + S^{(2)}_{2k;2,0}\ . \end{aligned}$$

The exotic return statistics $S^{(1)}$ and $S^{(2)}$ are the complicating features in the use of Proposition 6.1. As evidence, note that $S^{(1)}_{2k;k,0}$ is twice the number of returns of Dyck paths of length $2k$, $S^{(1)}_{2k+1;k,1}$ is worse again, and $S^{(2)}_{2k;k,0}$ is yet more complex. We can solve some simple cases arising from empty sums: $S^{(1)}_{n;c,p} = 0$ when $c \le 0$ or $p < 0$ or $n - p$ is odd or $n - p < 2c$; and $S^{(2)}_{n;c,p} = 0$ when $c \le 1$ or $p \le 0$ or $n - p$ is odd or $n - p < 2c$; in particular, $S^{(1)}_{n;c,n} = 0 = S^{(2)}_{n;c,n} = S^{(2)}_{n;c,n-2}$. There is also simplification when p is large relative to n.

Proposition 6.3. (i) For $n \ge 2$, $S^{(1)}_{n;1,n-2} = 2$.
For $n \ge 5$,
(ii) $S^{(1)}_{n;1,n-4} = 4n - 8$,
(iii) $S^{(1)}_{n;2,n-4} = 2n - 2$, and
(iv) $S^{(2)}_{n;2,n-4} = 2$.

Proof. First note that each 2-cycle LLT is worth 2 to $S^{(1)}$ and a 4-cycle counts for 3; a pair of side-by-side 2-cycles LLT is worth 4 to $S^{(2)}$.
(i) The only $\alpha \in E_{n;1,n-2}$ which contributes to $S^{(1)}$ has a 2-cycle LLT.
(ii) Here is a list of all the kinds of contributors: a 4-cycle LLT (two orientations, 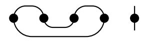 $\sim$ and 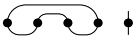 $\sim$, each with partial sum 3); a 2-cycle LLT on vertices 1 and 2, and one path of length 2, for example  $\sim$, which has 2 orientations and $n - 4$ locations possible, so partial sum $2 \times 2(n - 4)$; a 2-cycle on vertices 3 and 4, a 2-path (the LT) on vertices 1, 2 and 5 (two orientations, each contributing 1) and the remainder 0-paths, for example 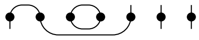 $\sim$, with partial sum 2. Thus $S^{(1)} = 6 + 4(n - 4) + 2 = 4n - 8$.
(iii) Here there must be two 2-cycles and $n - 4$ 0-paths. The contributing members have these configurations: two 2-cycles LLT, either side-by-side (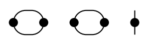 $\sim$, score 4) or concentric (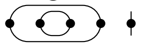 $\sim$, score 2), thus with partial sum 6; or one 2-cycle LLT on vertices $1, 2$, the LT on vertex 3, and the other 2-cycle on vertices $4, 5$ or $5, 6$ or $\ldots$, for example  $\sim$, giving $n - 4$ elements and a partial sum of $2(n - 4)$. Thus $S^{(1)} = 2n - 2$.
(iv) The only contribution to $S^{(2)}$ comes from the element with 2-cycles on vertices $1, 2$ and $3, 4$ and the remainder 0-paths, namely, $1 \cdot 1 + 1 \cdot 1 = 2$. □

An arithmetic progression can be seen in the depth $d = 1$ row of Table 5 (that is, $p = n - 2$). This is probably known by others who have studied $\mathscr{J}_n$, and may be proved by listing cases. We use Proposition 6.1 to provide a short proof of this result. Write ∇ for the backwards difference operator on sequences indexed by n, $\nabla : z_n \mapsto z_n - z_{n-1}$.

Proposition 6.4. For $n \ge 2$, $\quad e_{n;\cdot,n-2} = 3n - 5$.

Proof. Applying the constraint $c \le \frac{1}{2}(n - p)$, we find $c \le 1$, and for $c = 0, 1$ respectively, we have

$$\begin{aligned} e_{n;0,n-2} &= \ 0 + e_{n-1;0,n-3} + S^{(1)}_{n-1;1,n-3} + 0 &&= e_{n-1;0,n-3} + 2, \\ e_{n;1,n-2} &= \ e_{n-1;0,n-1} + e_{n-1;1,n-3} + 0 + 0 &&= 1 + e_{n-1;1,n-3}, \end{aligned}$$

for $n \ge 3$. Then summing over c, we find $e_{n;\cdot,n-2} = e_{n-1;\cdot,n-3} + 3$ or $\nabla e_{n;\cdot,n-2} = 3$. Solving, $e_{n;\cdot,n-2} - e_{2;\cdot,0} = \sum_{i=3}^{n} i3 = 3(n - 2)$ and by inspection, $e_{2;\cdot,0} = 1$, so $e_{n;\cdot,n-2} = 3n - 5$. Note the equation is true for $n \ge 2$. □

We can similarly use Propositions 6.1 and 6.3 to count idempotents of depth 2, that is, having $p = n - 4$.

Proposition 6.5. For $n \ge 5$, $\quad e_{n;\cdot,n-4} = \frac{n}{2}(9n - 35)$.

Proof. Here the only possibilities are $c \in \{0, 1, 2\}$. For brevity we set

$$z_n := e_{n;\,\cdot,n-4} = \sum_{c=0,1,2} e_{n;c,n-4}.$$

Now from Proposition 6.1 we have, for $n \geq 6$,

$$\begin{aligned}
e_{n;0,n-4} &= \quad 0 \quad &+ e_{n-1;0,n-5} + S^{(1)}_{n-1;1,n-5} + S^{(2)}_{n-1;2,n-5}, \\
e_{n;1,n-4} &= e_{n-1;0,n-3} &+ e_{n-1;1,n-5} + S^{(1)}_{n-1;2,n-5} + 0, \\
e_{n;2,n-4} &= e_{n-1;1,n-3} &+ e_{n-1;2,n-5} + 0 + 0.
\end{aligned}$$

Summing and using Proposition 6.3, we have

$$\begin{aligned}
z_n &= e_{n-1;\,\cdot,n-3} + z_{n-1} + 6(n-1) - 10 + 2, \\
\text{so that } \nabla z_n &= 3(n-1) - 5 + 6n - 14 = 9n - 22. \\
\text{Then } z_n - z_5 &= \sum_{i=6}^{n} (9i - 22) = \frac{9}{2}(n+6)(n-5) - 22(n-5).
\end{aligned}$$

But $z_5 = e_{5;\,\cdot,1} = C_3^2 = 25$, so the claim follows. □

The linearity in n of counts of idempotents at depth 1 and the quadratic dependence at depth 2 are generalised in Proposition 6.7 to depth k. The proof requires a preliminary result, which employs the concept of a *convex component* of α, defined as a minimal union of components which uses consecutive vertices. (For example, 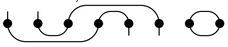 has two convex components, on the vertex sets $\{1, \ldots, 6\}$ and $\{7, 8\}$ respectively.) Moreover, we say that two convex components are *isomorphic* if they are identical except for a translation of the vertex numbering, as are the two convex components in 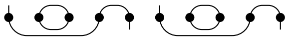 but not in 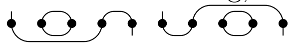.

Proposition 6.6. For fixed k and $n \geq 3k - 1$,

$$S^{(1)}_{n;\,\cdot,n-2k} = \frac{2 \cdot 3^{k-1}}{(k-1)!} n^{k-1} + O(n^{k-2}) \quad \text{and} \quad S^{(2)}_{n;\,\cdot,n-2k} = \frac{2 \cdot 3^{k-2}}{(k-2)!} n^{k-2} + O(n^{k-3}) \text{ as } n \to \infty.$$

Proof. Take $\alpha \in E_{n;\,\cdot,n-2k}$, and let $\mathscr{A}$ be the union of the convex components of α to the left of and including the leftmost transversal (LILT); $\mathscr{A}$ determines the contribution $\sigma(\mathscr{A})$ of α to $S^{(i)}_{n;\,\cdot,n-2k}$, independently of n. Now consider the set of all elements with a fixed configuration $\mathscr{A}$, which we may think of as a *macrostate*. We shall partition this set into *microstates* as next described. Let the convex components of α to the right of $\mathscr{A}$ be partitioned into isomorphism classes (some empty) A_ι, for $\iota \in I$, an index set excluding 0 and containing $1, 2, 3, 3'$ and other unspecified symbols. We shall specify that A_1 contains precisely all 0-paths (that is, all singleton components), that all 2-cycles on adjacent vertices make up A_2, and that there are two classes of convex components using three vertices, A_3 and $A_{3'}$, which contain 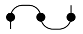 and 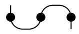 respectively. We write $a_\iota = |A_\iota|$ and say that two idempotents belong to the same microstate if they share the LILT $\mathscr{A}$ and their sequences (a_ι) are equal. Naturally the a_ι satisfy constraints. Let the number of vertices in $\mathscr{A}$ be L, and let v_ι represent the number of vertices in any element (a convex component) of A_ι. Then

$$\sum v_\iota a_\iota = n - L = \sum a_\iota + \sum_{\iota \neq 1} (v_\iota - 1) a_\iota. \tag{11}$$

Let J be the subset of I indexing all the classes with components having at least one path (so $1, 3, 3', \dots \in J$). Since there are $n - 2k$ paths, and $\mathscr{A}$ contains at least one,

$$\sum_{\iota \in J} a_\iota \leq n - 2k - 1.$$

The point of all this is that the number of idempotents in a microstate (a_ι) is given by the multinomial coefficient

$$\frac{(a_1+a_2+\cdots)!}{a_1!a_2!\cdots} = \frac{\{n-L-\sum_{\iota\neq 1}(v_\iota-1)a_\iota\}^{[a_2+a_3+a_{3'}+\cdots]}}{a_2!a_3!\cdots},$$

where equation (11) is used, and $x^{[y]}$ means the descending factorial of y factors. Thus to find the term in $S^{(i)}$ of highest degree in n, we encounter the integer programming problem

$$\begin{aligned} \text{maximise } z &= \sum_{\iota\neq 1} a_\iota \\ \text{subject to } \sum v_\iota a_\iota &= n-L, \\ \sum_{\iota\in J} a_\iota &\leq n-2k-1. \end{aligned}$$

Now $v_\iota = \iota$ for $\iota \in \{1,2,3\}$ and $v_{3'} = 3$. A feasible solution in which there is some convex component in an A_ι with $v_\iota \geq 4$ may be replaced by two or more convex components using more paths or the same number of paths and some 2-cycles, improving the objective while preserving feasibility; the same is true of the LT. Thus solutions have $a_\iota = 0$ for $\iota \notin \{1,2,3,3'\}$, every path (including the LT) is either a 0-path or a 2-path, and the second constraint holds with equality. Moreover, $a_3 + a_{3'}$ may be treated as a single variable. Our problem thus reduces to

$$\begin{aligned} &\text{maximise } z = a_2 + (a_3+a_{3'}), \\ \text{subject to } \quad & a_1 + 2a_2 + 3(a_3+a_{3'}) = n-2\ell-1, \\ & a_1 + (a_3+a_{3'}) = n-2k-1, \end{aligned}$$

where we have also written $L = 2\ell+1$ for convenience. Then, provided $\ell \leq k$ and $n \geq 3k-\ell+1$, all solutions are given by

$$\begin{pmatrix} a_1 \\ a_2 \\ a_3+a_{3'} \end{pmatrix} = \begin{pmatrix} n-2k-1-t \\ k-\ell-t \\ t \end{pmatrix}, \tag{12}$$

for $0 \leq t \leq k-\ell$. The objective value is $k-\ell$, so we should choose ℓ minimal subject to $\sigma(\mathscr{A}) \neq 0$, which is $\ell = 1$ for $S^{(1)}$ and $\ell = 2$ for $S^{(2)}$. Thus the microstates contributing the highest order terms to $S^{(i)}$ are identified. Moreover, $\sigma(\mathscr{A}) = 2$ in both cases. It remains to count the idempotents (interface graphs) that have ℓ 2-cycle convex components on the vertex set $\{1,\ldots,2\ell\}$, a LT on vertex $\{2\ell+1\}$, and satisfy (12). This number is the sum of multinomial coefficients

$$\sum_{t=0}^{k-\ell}\sum_{a_3+a_{3'}=t}\frac{(n-k-\ell-t-1)!}{(n-2k-t-1)!\;a_2!\;a_3!\;a_{3'}!} = \sum_{t=0}^{k-\ell}\sum_{a_3+a_{3'}=t}\frac{(n-k-\ell-t-1)^{[k-\ell]}}{(k-\ell-t)!\;a_3!\;a_{3'}!},$$

and we need to select those that contribute to the leading term. The coefficient of the term in $n^{k-\ell}$ is $\sum_{t=0}^{k-\ell}\sum_{a_3+a_{3'}=t}\frac{1}{(k-\ell-t)!\;a_3!\;a_{3'}!}$. To evaluate this, note that

$$\frac{(k-\ell)!}{(k-\ell-t)!\;a_3!\;a_{3'}!}$$

is the coefficient of $x^{k-\ell-t}(y+z)^t$ in the expansion of $\{x+(y+z)\}^{k-\ell}$, and so

$$\sum_{t=0}^{k-\ell}\sum_{a_3+a_{3'}=t}\frac{1}{(k-\ell-t)!\;\;a_3!\;a_{3'}!} = \frac{3^{k-\ell}}{(k-\ell)!}.$$

The assertions of the rubric follow on multiplication by $\sigma(\mathscr{A}) = 2$. □

It follows that $\nabla^{k-1}S^{(1)}_{n;\cdot,n-2k} = 2\cdot 3^{k-1}$ and $\nabla^{k-1}S^{(2)}_{n;\cdot,n-2k} = 0$ for $n \geq 3k-1$. This gives a result about counts of idempotents of depth k which is evident in the data of Table 3. We remark that there also seem to be similar patterns in the Motzkin table (Table 2).

Proposition 6.7. For fixed k and $n \geq 3k-1$, $\nabla^k e_{n;\cdot,n-2k} = 3^k$.

Proof. Let $z_n^{(k)} = e_{n;\cdot,n-2k}$, and assume for the purpose of induction that $\nabla^{k-1}z_n^{(k-1)} = 3^{k-1}$, as indeed holds for $k = 2$ by Proposition 6.4. Then by Proposition 6.1 we have

$$\begin{aligned} e_{n;\cdot,n-2k} &= e_{n-1;\cdot,n-1-2(k-1)} + e_{n-1;\cdot,n-2k-1} + S^{(1)}_{n-1;\cdot,n-2k-1} + S^{(2)}_{n-1;\cdot,n-2k-1}, \\ \text{that is, } z_n^{(k)} &= z_{n-1}^{(k-1)} + z_{n-1}^{(k)} + S^{(1)}_{n-1;\cdot,n-1-2k} + S^{(2)}_{n-1;\cdot,n-1-2k}, \end{aligned}$$

and so

$$\nabla z_n^{(k)} = z_{n-1}^{(k-1)} + S^{(1)}_{n-1;\cdot,n-1-2k} + S^{(2)}_{n-1;\cdot,n-1-2k}.$$

Now applying the inductive hypothesis and using Proposition 6.6,

$$\begin{aligned} \nabla^k z_n^{(k)} &= \nabla^{k-1} z_{n-1}^{(k-1)} + \nabla^{k-1}\{S^{(1)}_{n-1;\cdot,n-1-2k} + S^{(2)}_{n-1;\cdot,n-1-2k}\} \\ &= 3^{k-1} + 2\cdot 3^{k-1} + 0 \\ &= 3^k, \end{aligned}$$

as claimed. □

Further progress on these topics—especially, perhaps, asymptotics for e_n—seems to require a better combinatorial understanding of the return statistics $S^{(1)}$ and $S^{(2)}$. There are connections between these statistics and the Kauffman idempotent numbers, reminiscent of the meandric numbers: from Proposition 4.4 (iii), we have $|E(\mathscr{J}_n^{\xi})| = e_{n;0,\cdot} := \sum_p e_{n;0,p}$. Then from Proposition 6.1 we have

$$\begin{aligned} e_{n;0,\cdot} &= 0 + e_{n-1;0,\cdot} + S^{(1)}_{n-1;1,\cdot} + S^{(2)}_{n-1;2,\cdot}\,, \\ \text{giving} \qquad \nabla e_{n;0,\cdot} &= S^{(1)}_{n-1;1,\cdot} + S^{(2)}_{n-1;2,\cdot}\,. \end{aligned}$$

Finally, that there is more to be discovered about the series of fascinating semigroups $\mathscr{J}_n$ and their relatives is strongly indicated by Figures 4 and 5, which present eggbox diagrams in which the $\mathscr{H}$-classes are shaded if they contain an idempotent. The interested reader may consult Larsson's thesis [15] or the article of Lau and FitzGerald [16] for more on the $\mathscr{D}$-structure of $\mathscr{J}_n$. The bitmaps here were created by Dr A. Egri-Nagy from $\mathscr{D}$-class tables generated using the Semigroups package for GAP [19]; we thank him for sharing them. The reader who wishes to see more is referred to East *et alii* [5].

Acknowledgement. The authors express their thanks to Dr Phillip Edwards for earlier contributions to this project, especially concerning combinatorial interpretation of the $\mathscr{D}$-structure of the Jones monoids, and Dr Attila Egri-Nagy for emphasising the possible significance of the self-similarity evident in the eggbox diagrams of Figures 4 and 5. The first author (ID) acknowledges the support of Grant No.174019 of the Ministry of Education, Science and Technological Development of the Republic of Serbia, and Grant No.0851/2015 of the Secretariat of Science and Technological Development of the Autonomous Province of Vojvodina. Essential parts of the exposition were developed during NL's side-trip to Hobart, which was assisted by the School of Physical Sciences of the University of Tasmania. Discussions, comments, corrections, sketches, code- and file-sharing between the authors were all facilitated by a popular social-media platform, for which we say: *Like!*

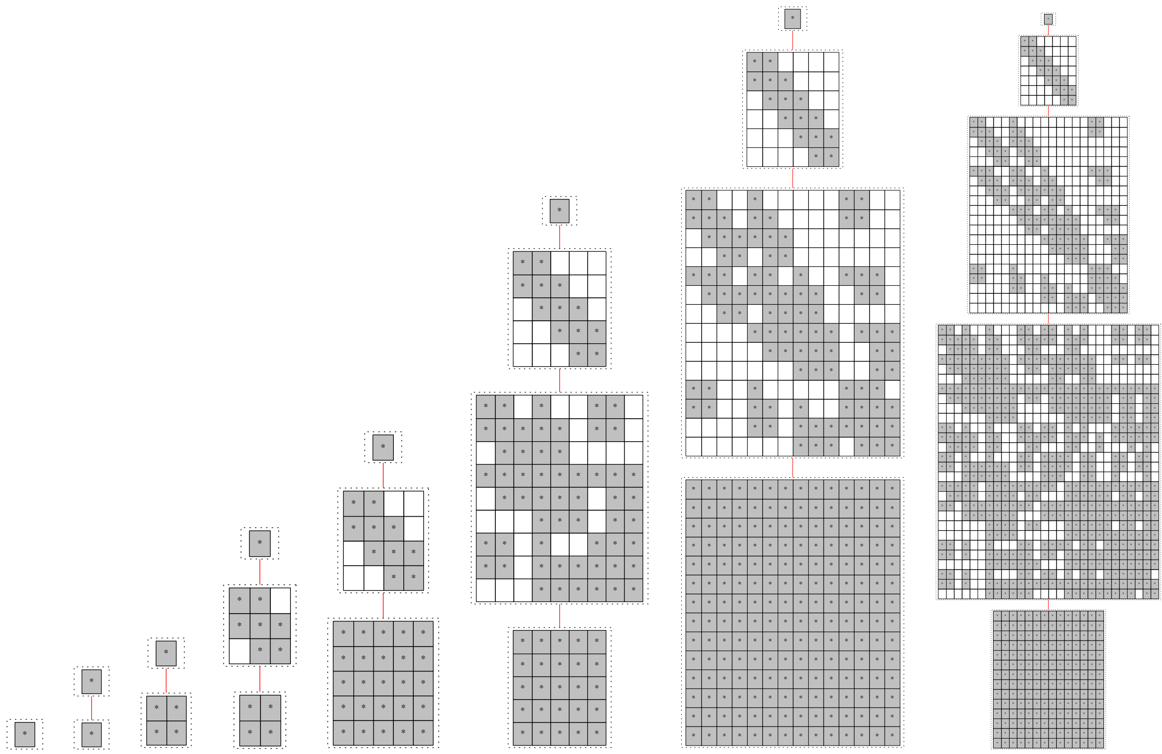

Figure 4: Eggbox diagrams of the Jones monoids $\mathscr{J}_n$ for $1 \leq n \leq 8$.

References

[1] Benkart, G. M., Halverson, T.: Motzkin algebras. European J. Combin. **36**, 473–502 (2014)

[2] Borisavljević, M., Došen, K., Petrić, Z.: Kauffman monoids. J. Pure Appl. Algebra **184**, 7–39 (2003)

[3] Deutsch, E.: Dyck path enumeration. Discrete Math. **204**, 167–202 (1999)

[4] Dolinka, I., East, J., Evangelou, A., FitzGerald, D., Ham, N., Hyde, J., Loughlin, N.: Enumeration of idempotents in diagram semigroups and algebras. J. Combin. Theory Ser. A **131**, 119–152 (2015)

[5] East, J., Egri-Nagy, A., Francis, A. R., Mitchell, J. D.: Finite diagram semigroups: extending the computational horizon. Preprint, `arXiv:1502.07150v2`

[6] The GAP Group: GAP – Groups, Algorithms, and Programming, Version 4.7.7(2015). `http://www.gap-system.org`

[7] Halverson, T., Ram, A.: Partition algebras. European J. Combin. **26**, 869–921 (2005)

[8] Hatch, K., Ly, M. and Posner, E.: Presentation of the Motzkin monoid. Preprint, (2013). `arXiv:1301.4518v1`

[9] Higgins, P. M.: Techniques of Semigroup Theory. Oxford Science Publications, The Clarendon Press, Oxford Univ. Press, New York (1992)

[10] Howie, J. M.: Fundamentals of Semigroup Theory. London Math. Soc. Monogr. (N.S.) 12, Oxford Univ. Press, New York (1995)

[11] Jackson, M. G. (ed.): General Algebra and Its Applications 2013: Problem Session. Algebra Universalis **74**, 9–16 (2015)

[12] Jones, V. F. R.: Index for subfactors. Invent. Math. **72**, 1–25 (1983)

[13] Jones, V. F. R.: The Potts model and the symmetric group. In Subfactors: Proceedings of the Taniguchi Symposium on Operator Algebras (Kyuzeso, 1993), World Sci. Publishing, River Edge, NJ, 259–267 (1994)

[14] Kauffman, L. H.: An invariant of regular isotopy. Trans. Amer. Math. Soc. **318**, 417–471 (1990)

[15] Larsson, D.: Combinatorics on Brauer-type semigroups, U.U.D.M. Project Report 2006:3 (2006). `http://www.diva-portal.org/smash/get/diva2:305049/FULLTEXT01.pdf`

[16] Lau, K. W., FitzGerald, D. G.: Ideal structure of the Kauffman and related monoids. Comm. Algebra **34** (7), 2617–2629 (2006)

[17] Legendre, S.: Foldings and meanders. Australas. J. Combin. **58**, 275–291 (2014)

[18] Martin, P. P.: Temperley-Lieb algebras for nonplanar statistical mechanics—the partition algebra construction. J. Knot Theory Ramifications **3**, 51–82 (1994)

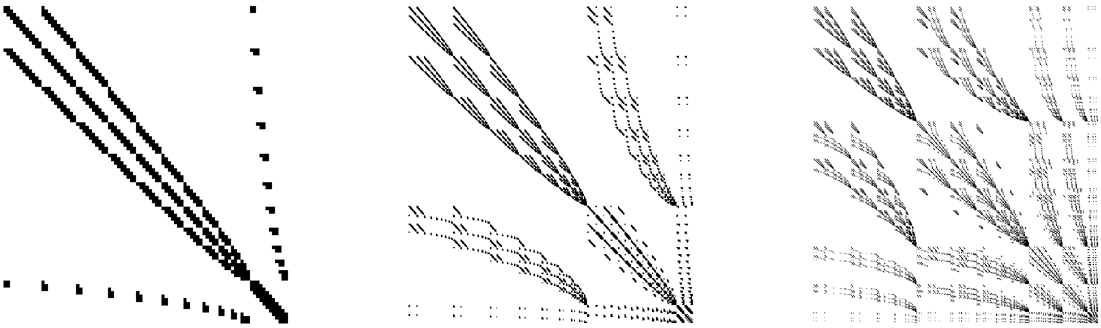

Figure 5: Three $\mathscr{D}$-classes from the Jones monoid $\mathscr{J}_{15}$.

[19] Mitchell, J. D. et al.: `semigroups -- a GAP package, v. 2.2` (2015). `http://www-groups.mcs.st-andrews.ac.uk/~jamesm/semigroups.php`

[20] Sloane, N. J. A.: The Online Encyclopedia of Integer Sequences. `http://www.oeis.org`

[21] Temperley, H. N. V., Lieb, E. H.: Relations between the "percolation" and "colouring" problem and other graph-theoretical problems associated with regular planar lattices: some exact results for the "percolation" problem. Proc. Roy. Soc. London Ser. A **322**, (1549) 251–280 (1971)

A Appendix: Algorithms

The formulæ in Corollary 3.6 and equation (6) are amenable to parallel computation. Here we sketch an algorithm for the computation of the idempotent numbers by the method of Section 3. There is wide scope for choice of methods to represent and sequentially generate Dyck and Motzkin semi-words and perhaps also to identify components and count returns—inspiration may be found in Deutsch's article [3] and its bibliography—so we do not trouble with those details here.

Outline of a general algorithm. Input n, the number of vertices. Partition the $\mathscr{R}$-classes of D, given by Motzkin or Dyck semi-words or words of length n, into k parts, say $R_1 \dots R_k$. A 'secretary' or master processor $\mathcal{P}_0$ passes R_j (or sufficient information to sequentially generate it) to Processor $\mathcal{P}_j$.

- For each $\upsilon \in R_k$, $\mathcal{P}_j$ runs through all the $\mathscr{L}$-classes of D, indexed by Motzkin or Dyck n-words λ of matching rank 0 or 1, calculating as follows.
  - Concatenate to form the pair (υ, λ), representing δ as in representation(iv) of Section 2.1, checking for idempotency if $\text{rank}(\delta) = 1$. Identify the levels, edges, returns and components of δ as in Table 1.
    - For each cycle component θ, count the returns and calculate $x_\theta = u_\theta l_\theta$, and then update $P = \prod(1 + x_\theta)$ and $K = \prod x_\theta$. (Note that if θ has no returns on at least one side, $K = 0$ and P is unchanged.) It could also store

$$S_1 = \sum x_\theta, \quad S_2 = \sum_{\theta_1 < \theta_2} x_{\theta_1} x_{\theta_2}, \text{ etc.}$$

    When all (necessary) components are done (dependent on parity), $\mathcal{P}_j$ adds P, K and the S_i to accumulators and goes to the next concatenation $\delta' = \upsilon\lambda'$ ($' =$ successor) and repeats.

  When the $\mathscr{L}$-classes are all finished, $\mathcal{P}_j$ increments the prefix υ and repeats. When it has done all members of its domain R_j, it returns the accumulated values P, K, and S_i to the secretary.

When all parts of D are finished, the secretary processor reports the results e_n, etc.

Code for methods used in comparison of times in Tables 6 and 7. Method 1 is a 'brute force' application of GAP, and ran out of memory at $n = 10$:

```
B := [ ];
n := 1; Size( Idempotents( MotzkinMonoid( n ) ) );; t := time;; Add( B, t );;
n := n+1; Size( Idempotents( MotzkinMonoid( n ) ) );; t := time;; Add( B, t );; # execute
```

```
this line as often as desired
B;
```

Method 2 (dubbed ‘memoryless’) checks element-wise and accumulates:

```
MotzCount := function( n )
local count, Mn, s;
count := 0;
Mn := MotzkinMonoid( n );
for s in Iterator( Mn ) do
if s^2 = s then
count := count + 1;
fi;
od;
return count;
end;
A := [ ];
n := 1;; MotzCount(n);; t := time;; Add( A, t );;
n := n+1; MotzCount(n);; t := time;; Add( A, t );; # again, repeat this
A;
```